

1 *Author Comments: Response to reviewers' comments*

2

3 Title: Evaluation on the effect of regional joint control measures in changing photochemical  
4 transformation: A comprehensive study of the optimization scenario analysis

5

6 The manuscript investigates the effectiveness of the emission control to the pollutant concentrations  
7 during the 2nd World Internet Conference from December 16 to December 18, 2015. The authors have  
8 addressed reviewers' points and make recommended changes in the manuscripts. The manuscript is well-  
9 organized. I suggest this manuscript goes through minor revision with the following comments.

10 We would like to take this opportunity to express our sincere thanks the anonymous reviewers for the  
11 comments and suggestions, which have helped greatly to improve this paper.

12 Minor points:

13

14 1. How do you conduct the emission inventory to account for the controlled measures?

15 **Firstly, we have developed a basic emission inventory for the YRD region based on a bottom**  
16 **up methodology with activity data, emission factors and control technologies as inputs.**  
17 **Secondly, we further developed a controlled emission inventory to account for the measures**  
18 **based on the emission reduction requirements described in the control measures plan.**

19 Based on the control measures plan, three provinces and Shanghai municipality in the YRD region  
20 carried out joint control measures and three kind of areas with different emission reduction  
21 requirements were established, including (i)key areas, (ii)strict control areas, (iii)control areas and  
22 extension areas, respectively. Among them, key areas and strict control areas included Zhejiang  
23 province (including Hangzhou, Ningbo, Huzhou, Jiaxing and Shaoxing), Shanghai (including Jinshan  
24 and Fengxian), Jiangsu province (including Suzhou and Wuxi) and Anhui province (including  
25 Xuancheng, Ma'anshan and Wuhu). The following measures were taken in the key areas and control  
26 areas: (1) Strictly control emissions from coal-burning power plants: reduce emissions from power  
27 plants which have not completed ultra-low emission transmission processes by 50% in key areas and  
28 by 30% in control areas. (2) Reduce emissions from key facilities: restriction or suspension of  
29 production were imposed on industries including cement, steel, construction materials,  
30 petrochemicals, chemicals, casting, leather, non-ferrous metals, plate glass, pharmaceuticals, surface

31 spraying and printing. Activities from all key facilities in the key areas were suspended (maximum  
32 production limits were imposed on steel and petrochemical industries), while activities from key  
33 facilities in the control areas were reduced by 30%. Facilities which could not meet the emission  
34 standards in a stable way, or facilities that are not equipped with exhaust gas treatment or the exhaust  
35 gas treatment equipment cannot operate normally were suspended. Operation and/or maintenance at  
36 petrochemical and chemical facilities were prohibited. (3) Strictly control motor vehicle emissions:  
37 in the core areas of Zhejiang province, motor vehicle restrictions were implemented, which means  
38 that low-speed trucks were prohibited to pass except for people's livelihood-related activities.  
39 Vehicles which had not obtained valid qualifications for environmental inspection were prohibited  
40 for operation. (4) Control dust emissions: Activities at construction sites were suspended in the key  
41 areas and control areas. Dust materials were prohibited to be transported within key neighbourhoods.  
42 Dust control measures were implemented on renovation operations at ports, docks, railway stations  
43 and commercial concrete mixing stations and at materials storage yards. (5) Control emissions from  
44 other sources: in the key areas and control areas, oil storage facilities, gas stations or tank trucks  
45 which were not equipped with equipment for oil and gas recycling or equipment that could not operate  
46 normally were prohibited for trade or transporting oil products. Outdoor barbecue, burning activities  
47 in the open air were prohibited. All the primary schools, secondary schools, kindergartens, institutions  
48 and public institutions in Jiaxing were given a three-day vacation. **Based on the emission reduction  
49 ratio and suspended emission sources including both industries and fugitive emissions, we  
50 estimated the emissions reductions.**

51 In addition, during the campaign, some cities took stricter emission reduction measures for predicted  
52 possible upcoming severe air pollution events. Shanghai started temporary control of heavy pollution  
53 on December 14 and initiated the yellow warning for heavily polluted weather on December 15.  
54 Emergency control measures were initiated on December 15 with strengthening control efforts for  
55 industries, work sites and motor vehicles. **For these urgent control measures, we further  
56 calculated emissions reductions and consolidated into the controlled emissions inventory.**

57 **Based on the control measures and emission reduction requirements mentioned above, we  
58 developed a controlled emission inventory to account for the control measures.**

59 [Changes in manuscript:](#)

60 In the end of Section 2.3.1, we inserted the following descriptions regarding the emissions inventory  
61 accounting for control measures:

62 We further developed a controlled emission inventory to account for the control measures based on  
63 the emission reduction requirements described in the control measures plan and the control measures  
64 for the emergency air pollution warning. These estimates are basically according to the control  
65 measures and reduction requirements for specific source sectors and cities described the control plan.

66 2. What is the difference between your findings and previous studies?

67 China has successfully implemented air pollution control plans and ensured good air quality for  
68 several mega events. After implementation of these control measures, it is important to understand  
69 how effective these strategies are. Previous studies mainly reported the effects of those control  
70 measures on the air quality based on observations, emissions or simulations. For example, Lu et al  
71 (2016) reported the influence of control measures on air quality during the second Asian Youth  
72 Games in Nanjing based on measurements of 15 trace metal elements. Tang et al (2015) reported the  
73 impact of emission controls on air quality in Beijing during APEC based on lidar ceilometer  
74 observations. Liu et al., (2013) reported the emission controls and changes in air quality in Guangzhou  
75 during the Asian Games based on combination of observation data, emission reduction measures and  
76 air quality simulations. Han et al., (2016) reported the effect of the pollution control measures on  
77 PM<sub>2.5</sub> during the 2015 China Victory Day Parade based on measurements, and found that the decrease  
78 in concentration of water-soluble ions in PM<sub>2.5</sub>, which results from variations in air mass transport.  
79 Wang et al., (2016) reported the relative impact of emissions controls and meteorology on air pollution  
80 mitigation associated with the Asia-Pacific Economic Cooperation (APEC) conference in Beijing, China;  
81 they used PMF to analyse changes of the sources. Wang et al., (2015) summarized the atmospheric  
82 composition changes before and during the APEC period for four stages from 20 October to 20 November  
83 2014; they also assessed the change in atmospheric composition after the implementation of various  
84 control measures on a regional scale. Of the previous studies, changes of chemistry before, during and  
85 after these mega events are seldom discussed. This study reports the changes of compositions and  
86 chemistry from these combined analyses. These are the main difference. Since we do not have similar or  
87 different results to compare, we did not insert these contents into the manuscript.

88 References:

89 Han, X. K., Guo, Q. J., Liu, C. Q., et al.: Effect of the pollution control measures on PM<sub>2.5</sub> during the 2015 China Victory  
90 Day Parade: Implication from water-soluble ions and sulfur isotope, *Environ. Pollut.*, 218, 230-241, 2016.

91 Liu, H., Wang, X. M., Zhang, J. P., et al.: Emission controls and changes in air quality in Guangzhou during the Asian  
92 Games, *Atmos. Environ.*, 76, 81-93, 2013.

93 Lu, Q., Zhang, Y. F., Ma, Y. H., et al.: Source identification of trace elements in the atmosphere during the second Asian  
94 Youth Games in Nanjing, China: Influence of control measures on air quality, *Atmos. Pollut. Res.*, 7 (3), 547-556, 2016.

95 Tang, G., Zhu, X., Hu, B. M. et al.: Impact of emission controls on air quality in Beijing during APEC 2014: lidar ceilometer  
96 observations, *Atmos. Chem. Phys.*, 15, 12667-12680, 2015.

97 Wang, Y. Q., Zhang, Y., Schauer, J. J., et al.: Relative impact of emissions controls and meteorology on air pollution  
98 mitigation associated with the Asia-Pacific Economic Cooperation (APEC) conference in Beijing, China, *Sci. Total  
99 Environ.*, 571, 1467-1476, 2016.

100 Wang, Z. S., Li, Y. T., Chen, T., et al.: Changes in atmospheric composition during the 2014 APEC conference in Beijing,  
101 *J. Geophys. Res.*, 120 (24), 2015.

102 3. Line 106: “big different effects” to “significantly different effects”

103 Revised.

104 4. Line 423: “The chemistry also changes ...”, do you mean the “chemical composition of PM<sub>2.5</sub> also  
105 changes...” or “chemical processes associated PM<sub>2.5</sub> production”.

106 By saying “The chemistry also changes...”, we mean both the chemical compositions of PM<sub>2.5</sub> and  
107 chemical processes associated with PM<sub>2.5</sub> production change, which can be shown by the following  
108 interpretations including changes of concentrations and the difference of SNA formation.

109 Changes in manuscript:

110 Both the chemical compositions of PM<sub>2.5</sub> and chemical processes associated with PM<sub>2.5</sub> production change  
111 if we compare observed data during and after the regulation.

112

113 **Evaluation on the effect of regional joint control measures in changing**  
114 **photochemical transformation: A comprehensive study of the optimization**  
115 **scenario analysis**

116 Li LI<sup>1,2#</sup>, Shuhui ZHU<sup>2#</sup>, Jingyu AN<sup>2#</sup>, Min ZHOU<sup>2</sup>, Hongli WANG<sup>2\*</sup>, Rasha YAN<sup>2</sup>, Liping QIAO<sup>2</sup>, Xudong TIAN<sup>3</sup>,  
117 Lijuan SHEN<sup>4</sup>, Ling Huang<sup>1</sup>, Yangjun Wang<sup>1</sup>, Cheng Huang<sup>2\*</sup>, Jeremy C AVISE<sup>5</sup>, Joshua S FU<sup>6</sup>

- 118 1. School of Environmental and Chemical Engineering, Shanghai University, Shanghai, 200444, China  
119 2. State Environmental Protection Key Laboratory of the Cause and Prevention of Urban Air Pollution Complex, Shanghai Academy  
120 of Environmental Sciences, Shanghai 200233, China  
121 3. Zhejiang Environmental Monitoring Center, Hangzhou, 310014, China  
122 4. Jiaxing Environmental Monitoring Station, Jiaxing, 314000, China  
123 5. Laboratory for Atmospheric Research, Washington State University, Pullman, Washington, USA.  
124 6. Department of Civil & Environmental Engineering, University of Tennessee, Knoxville, TN 37996, USA

125  
126 \*Correspondence to: C. Huang (huangc@saes.sh.cn), H. L. WANG (wanghl@saes.sh.cn) and L. Li  
127 (Lily@shu.edu.cn)

128 #These three people contributed equally to this work.  
129

130 **Abstract:** Heavy haze usually occurs in winter in eastern China. To control the severe air pollution during the season,  
131 comprehensive regional joint-control strategies were implemented throughout a campaign. To evaluate the  
132 effectiveness of these strategies and to provide some insights into strengthening the regional joint-control  
133 mechanism, the influence of control measures on levels of air pollution were estimated with an integrated  
134 measurement-emission-modeling method. To determine the influence of meteorological conditions, and the control  
135 measures on the air quality, in a comprehensive study, the 2nd World Internet Conference was held during December  
136 16~18, 2015 in Jiaxing City, Zhejiang Province in the Yangtze River Delta (YRD) region. We first analyzed the air  
137 quality changes during four meteorological regimes; and then compared the air pollutant concentrations before,  
138 during and after the regulation under static meteorological conditions. Next, we conducted modeling scenarios to  
139 quantify the effects caused due to the air pollution control measures. We found that total emissions of SO<sub>2</sub>, NO<sub>x</sub>,  
140 PM<sub>2.5</sub> and VOCs in Jiaxing were reduced by 56%, 58%, 64% and 80%, respectively; while total emission reductions  
141 of SO<sub>2</sub>, NO<sub>x</sub>, PM<sub>2.5</sub> and VOCs over the YRD region are estimated to be 10%, 9%, 10% and 11%, respectively.  
142 Modelling results suggest that during the campaign from December 8 to December 18, PM<sub>2.5</sub> daily average  
143 concentrations decreased by 10 µg/m<sup>3</sup> with an average decrease of 14.6%. Our implemented optimization analysis  
144 compared with previous studies also reveal that local emission reductions play a key role in air quality improvement,  
145 although it shall be supplemented by regional linkage. In terms of regional joint control, to implement pollution  
146 channel control 48 hours before the event is of most benefit in getting similar results. Therefore, it is recommended  
147 that a synergistic emission reduction plan between adjacent areas with local pollution emission reductions as the  
148 core part should be established and strengthened, and emission reduction plans for different types of pollution  
149 through a stronger regional linkage should be reserved.

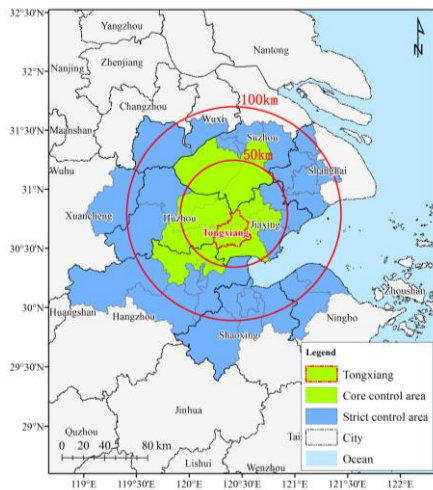
150 **Keywords:** PM<sub>2.5</sub>; regional joint control; YRD

151

## 152 1 Introduction

153 High concentrations of PM<sub>2.5</sub> has attracted much attention due to its impact on visibility (Pui et al., 2014),  
154 human health (West et al., 2016) and global environment. To control air pollution situation in China, the Ministry  
155 of Ecology and Environment of the People's Republic of China has released a lot of policies, which can generally  
156 be divided into long-term action plans (such as the Clean Air Action Plan (2013-2017), the Five-year Action Plans)  
157 and short-term control measures (such as Clean Air Protection during Mega Events, Air Pollution Warning and  
158 Protection Measures). China has successfully implemented some mega event air pollution control plans and ensured  
159 good air quality, including the 2008 Beijing Olympics (Kelly and Zhu, 2016); the 2010 World Expo in Shanghai  
160 (CAI-Asia, 2010); the 2010 Guangzhou Asian Games (Liu et al., 2013); the 2014 Asia-Pacific Economic  
161 Cooperation Forum (APEC) (Liang et al., 2017); 2014 Summer Youth Olympics in Nanjing (CAI-Asia, 2014) and  
162 the 2015 China Victory Day Parade (Victory Parade 2015) (Liang et al., 2017), etc. After implementation of these  
163 control measures, it is important to understand how effective these strategies are.

164 The 2<sup>nd</sup> World Internet Conference was held in Tongxiang, Jiaxing, Zhejiang during 16-18 December, 2015.  
165 To reduce air pollution during the conference, Zhejiang Province and the Regional Air-pollution Joint Control  
166 Office of the Yangtze River Delta (YRD) region developed an Action Plan for Air Pollution Control during the  
167 Conference (henceforth referred to as the Action Plan), which clarified target goals, time periods for implementing  
168 controls, regions in which the controls would be applied, and the control measures to be implemented, as described  
169 below. **Targets:** achieve an Air Quality Index (AQI) below 100 in “key areas”, an AQI below 150 in “control areas”,  
170 and to achieve significant improvement of the air quality in the surrounding (or buffer) regions outside the control  
171 areas. **Time Periods:** the time periods of interest for implementing various controls include the early stage (3 months  
172 before the conference), the advanced stage (2 weeks to 4 days before the conference) and the central stage (3 days  
173 before and 2 days after the conference). **Regions:** areas within a 50km radius, within a 100km radius and outside of  
174 a 100km radius from the centre of Tongxiang were classified as key areas, control areas and buffer areas,  
175 respectively. These areas cover 9 cities including Jiaxing, Huzhou, Hangzhou, Ningbo and Shaoxing in Zhejiang  
176 province, Suzhou and Wuxi in Jiangsu province and Xuancheng in Anhui province, as shown in Fig.1.



177  
178 Fig.1 Controlled regions in the Action Plan for Air Quality Control during the World Internet Conference

179 Many studies have provided descriptive analysis of changing concentrations of air pollutants during mega  
180 events; some have reported the emission reductions and related air quality changes (Wang, et al., 2009; Wang, et  
181 al., 2010; Liu, et al., 2013; Tang, et al., 2015; Li, et al., 2016; Wang, et al., 2016; Sun, et al., 2016; Wang, et al.,  
182 2015; Chen, et al., 2017; Han, et al., 2016; Qi, et al., 2016). However, different air pollution control targets, different  
183 control measures, and different locations, may cause big-significantly different effects among those strategies. In  
184 this paper, the reduction in PM<sub>2.5</sub> achieved through the Action Plan is investigated further to help quantify the level  
185 of PM<sub>2.5</sub> reduction that can be attributed to different aspects of the Action Plan. An integrated emission-  
186 measurement-modelling method described in the next section including analysis of multi-pollutant observations,  
187 backward trajectory and potential source contribution analyses, estimates of pollutant emission reductions, and  
188 photochemical model simulations were adopted to conduct a comprehensive assessment of the impact of control  
189 measures on air quality improvement based on three aspects: meteorological conditions, pollutant emission  
190 reductions of local sources, and regional contributions.

191 **2 Methodology**

192 In order to strengthen the regional air pollution joint-control mechanism in the YRD region, various measures  
193 and their implementation were systematically reviewed, and the qualitative and quantitative relationships among  
194 the implementation of measures, changes in emissions of air pollution sources and air quality improvement were  
195 studied. Specifically, the impact of measures such as management and control of coal-burning power plants,  
196 production restriction and suspension of industrial enterprises, motor vehicle limitation and work site suspension,

197 dust control were investigated. In addition, the role of meteorology (in particular, transport) was assessed in terms  
198 of its influence on the relevance and effectiveness of various measures, and ways of optimising air quality control  
199 measures and emergency emission reductions under heavy pollution during major events were evaluated.

200 To assess the effectiveness of the various controls outlined in the Action Plan, emission reductions associated  
201 with those controls were calculated, and photochemical modelling was conducted to determine the change in  $PM_{2.5}$   
202 attributed to specific controls. On this basis, an assessment of how to optimise control measures was carried out  
203 with respect to both the area in which the emission reduction took place, as well as the start time for implementing  
204 the controls (i.e., how far in advance do the controls need to be implemented). Analysis of the numerical modelling  
205 results is focused on the effectiveness of the control measures with respect to regional transport of pollutants in the  
206 YRD region.

## 207 **2.1 Measurements**

208 The On-line observational station was set up at the Shanxi supersite of Zhejiang Province (30.82 °N, 120.87  
209 °E), which was located at the core area for pollution-control measures. On-line hourly  $PM_{2.5}$  mass concentration,  
210 carbonaceous aerosols, elements, and ionic species were measured by the Synchronized Hybrid Ambient Real-time  
211 Particulate Monitor (SHARP, model 5030, Thermo Fisher Scientific Corporation, USA), the OC/EC carbon aerosol  
212 analyzer (Model-4, Sunset Laboratory Corporation, USA), the Xact multi-metals monitor (Xact<sup>TM</sup> 625, PALL  
213 Corporation, USA), and the Ambient Ion Monitor-Ion Chromatograph (AIM IC, model URG 9000, URG  
214 Corporation, USA), respectively. Meteorological parameters, including wind speed, wind direction, temperature,  
215 pressure, and relative humidity, were measured as well.

216  $PM_{2.5}$  concentration data quality conform to the standards of data quality control published by Ministry of  
217 Ecology and Environment of the People's Republic of China.

218 A semi-continuous Sunset OC/EC analyser was used to measure OC and EC mass loadings at the observation  
219 site by adopting NIOSH-5040 protocol based on thermal-optical transmittance (TOT). The ambient air was first  
220 sampled into a  $PM_{2.5}$  cyclone inlet with a flow rate of 8 L·min<sup>-1</sup>. The OC and EC were collected on a quartz fiber  
221 filter with an effective collection area of 1.13 cm<sup>2</sup>. The analyzer was programmed to collect aerosol for 45 min at  
222 the start of each hour, followed by the analysis of carbonaceous species during the remainder of the hour. The  
223 analysis procedure is described in detail by Huang et al. (2018)

224 The ionic concentrations of nitrate, sulphate, chloride, sodium, ammonium, potassium, calcium and  
225 magnesium ( $Na^+$ ,  $K^+$ ,  $Ca^{2+}$ ,  $NH_4^+$ ,  $Mg^{2+}$ ,  $NO_3^-$ ,  $SO_4^{2-}$ ,  $Cl^-$ ) in the fine fraction ( $PM_{2.5}$ ) were measured with a 1-hour  
226 time resolution using the AIM IC. The sample analysis unit is composed by an anion and a cation ion



227 chromatographs (Dionex ICS-1100), which was using guard columns with potassium hydroxide eluent (KOH) for  
228 the anion system and methane sulfonic acid (MSA) eluent for the cation system. The limit of the detection reported  
229 by the manufacturer is 0.1 ug/m<sup>3</sup> for all species. The operation principle of AIM-IC is described in detail by  
230 Markovic et al. (2012)

231 Hourly ambient mass concentrations of sixteen elements (K, Ca, V, Mn, Fe, As, Se, Cd, Au, Pb, Cr, Ni, Cu,  
232 Zn, Ag, Ba) in PM<sub>2.5</sub> were determined by the Xact multi-metals monitor. In brief, the Xact instrument samples the  
233 air through a section of filter tape at a flow rate of 16.7 lpm using a PM<sub>2.5</sub> sharp cut cyclone. The exposed filter tape  
234 spot then advances into an analysis area where the collected PM<sub>2.5</sub> is analyzed by energy-dispersive X-ray  
235 fluorescence (XRF) to determine metal mass concentrations. The sequence of sampling and analysis were performed  
236 continuously and simultaneously on an hourly basis.

## 237 2.2 Potential Source Contribution Analysis

238 TrajStat is a HYSPLIT model developed by Chinese Academy of Meteorological Sciences and NOAA Air  
239 Resources Laboratory based on geographic information system (GIS). It uses statistical methods to analyze air mass  
240 back trajectories to cluster trajectories and compute potential source contribution function (PSCF) with observation  
241 data and meteorological data included (Wang et al., 2009).

242 PSCF analysis is a conditional probability function using air mass trajectories to locate pollution sources. It  
243 can be calculated for each 1° longitude by 1° latitude cell by dividing the number of trajectory endpoints that  
244 correspond to samples with factor scores or pollutant concentrations greater than specified values by the number of  
245 total endpoints in the cell (Zeng et al., 1989). Therefore, pollution source areas are indicated by high PSCF values.  
246 Since the deviation of PSCF results could increase with the raise of distance between cell and receptor, therefore a  
247 weight factor ( $W_{ij}$ ) was adopted in this study to lower the uncertainty of PSCF results. PSCF and  $W_{ij}$  calculations  
248 are described in Eq. (1) and Eq. (2), where  $m_{ij}$  is the number of trajectory endpoints greater than specified values in  
249 cell (i, j),  $n_{ij}$  is the number of total endpoints in this cell (Zeng et al., 1989; Polissar et al., 1999).

$$250 \quad P = \frac{m_{ij}}{n_{ij}} \cdot W(n_{ij}) \quad (1)$$

$$251 \quad W(n_{ij}) = \begin{cases} 1.00, & 80 < n_{ij} \\ 0.70, & 20 < n_{ij} \leq 80 \\ 0.42, & 10 < n_{ij} \leq 20 \\ 0.05, & n_{ij} \leq 10 \end{cases} \quad (2)$$

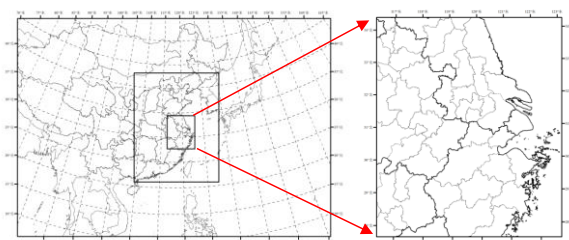
252 In this study, the TrajStat modelling system was used to analyze potential source contribution areas of PM<sub>2.5</sub>  
253 in Jiaying during different pollution episodes with the combination of Global Data Assimilation System (GDAS)  
254 meteorological data provided by the NCEP (National Center for Environmental Prediction). Polluted air mass

255 trajectories corresponded to those trajectories with  $PM_{2.5}$  hourly concentration higher than  $75 \mu g/m^3$ .

## 256 2.3 Model setup

### 257 2.3.1 Model selection and parameter settings

258 In this study, the WRF-CMAQ/CAMx air quality numerical modelling system was used to evaluate the  
259 improvement in air quality resulting from the control measures outlined in the Action Plan. It takes into account of  
260 modeling variations from different air quality models. For the mesoscale meteorological field, we adopted the WRF  
261 model Version 3.4 (<https://www.mmm.ucar.edu/wrf-model-general>), the CAMx model Version 6.1  
262 (<http://www.camx.com/>) and the CMAQ model Version 5.0 (Nolte et al., 2015; <http://www.cmascenter.org/cmaq/>).  
263 The chemical mechanism utilized in CMAQ was the CB05 gas phase chemical mechanism (Yarwood, et al., 2005)  
264 and AERO5 aerosol mechanism, which includes the inorganic aerosol thermodynamic model ISORROPIA (Nenes,  
265 et al., 1998) and updated SOA yield parameterizations. The gaseous and aerosol modules used in CAMx are the  
266 CB05 chemical mechanism and CF module, respectively. The aqueous-phase chemistry for both models is based  
267 on the updated mechanism of the Regional Acid Deposition Model (RADM) (Chang et al., 1987). Particulate Source  
268 Apportionment Technology (PSAT) coupled in the CAMx is applied to quantify the regional contributions to  $PM_{2.5}$   
269 as well. The WRF meteorological modeling domain consists of three nested Lambert projection grids of 36km-  
270 12km-4km, with 3 grids larger than the CMAQ/CAMx modeling domain at each boundary. WRF was run  
271 simultaneously for the three nested domains with two-way feedback between the parent and the nest grids. Both the  
272 three domains utilized 27 vertical sigma layers with the top layer at 100hpa, and the major physics options for each  
273 domain listed in Table 1. For the CMAQ/CAMx modelling domain shown in Figure 2, we adopted a 36-12-4km  
274 nested domain structure with 14 vertical layers, which were derived from the WRF 27 layers. The two outer domains  
275 cover much of eastern Asia and eastern China, respectively, while the innermost domain covers the YRD region.  
276 The simulation period was from 1-18 December, 2015, during which 1-7 December was utilized for model spin-up  
277 and 8-18 December was the key period for analysis of the modelling results with control measures.



278 Fig 2. Modeling domain  
279  
280

281

Table 1 Parameterization scheme of the physical processes in the WRF model

Physical Processes	Parameterization Scheme	Reference
Microphysical Process	Purdue Lin Scheme	(Lin, 1983)
Cumulus Convective Scheme	Grell-3 Scheme	(Grell and Dévényi, 2002)
Road Process Scheme	Noah Scheme	(Ek, 2003)
Boundary Layer Scheme	Yonsei University (YSU) Scheme	(Hong, 2006)
Long-wave Radiation	RRTM Long-wave Radiation Scheme	(Mlawer et al., 1997)
Short-wave Radiation Scheme	Goddard Short-wave Radiation Scheme	(Chou and Suarez, 1999)

282 Initial and boundary conditions (IC/BCs) for the WRF modeling were based on 1-degree by 1-degree grids  
 283 FNL Operational Global Analysis data that are archived at the Global Data Assimilation System (GDAS). Boundary  
 284 conditions to WRF were updated at 6-hour intervals for D01.

285 Anthropogenic source emission inventory in YRD is based on a most recent inventory developed by our group  
 286 (Huang et al., 2011; Li et al., 2011; Liu et al., 2018). The emission inventory for areas outside YRD in China is  
 287 derived from the MEIC model (Multi-resolution Emission Inventory of China, latest data for  
 288 2012(<http://www.meicmodel.org>) and anthropogenic emissions over other Asian region are from the MIX emission  
 289 inventory for 2010 (Li et al., 2017). Biogenic emissions are calculated by the MEGAN v2.1 (Guenther et al., 2012).

290 [We further developed a controlled emission inventory to account for the control measures based on the emission](#)  
 291 [reduction requirements described in the control measures plan and the control measures for the emergency air](#)  
 292 [pollution warning. These estimates are basically according to the control measures and reduction requirements for](#)  
 293 [specific source sectors and cities described the control plan.](#) The Sparse Matrix Operator Kernel Emissions (SMOKE,  
 294 <https://www.cmascenter.org/smoke>) model is applied to process these emissions for modeling inputs that is more  
 295 detailed emission processes and not usually used in China.

### 296 2.3.2 Model performance

297 Prior to evaluating the effectiveness of the control measures and reactions, the performance of the modelling  
 298 system was evaluated to ensure it was able to reasonably reproduce the observed meteorological conditions and  
 299 PM<sub>2.5</sub> levels. Statistical indexes used for model evaluation include Normalised Mean Bias (NMB), Normalised  
 300 Mean Error (NME) and Index of Agreement (IOA). The equations to calculate these statistical indexes are as follows:

$$NMB = \frac{\sum(P_j - O_j)}{\sum O_j} \times 100\% \quad (3)$$

$$NME = \frac{\sum |P_j - O_j|}{\sum O_j} \times 100\% \quad (4)$$

$$IOA = 1 - \frac{\sum(P_j - O_j)^2}{\sum(|P_j - \bar{O}| + |O_j - \bar{O}|)^2} \quad (5)$$

301 where  $P_j$  and  $O_j$  are predicted and observed hourly concentrations, respectively.  $\bar{O}$  is the average value of  
 302 observations. IOA ranges from 0 to 1, with 1 indicating perfect agreement between model and observation.

303 Observational data from the Shanxi supersite in Jiaxing City were compared with model results for model  
 304 evaluation verification. Table 2 shows the summary statistics for the main meteorological parameters simulated  
 305 with the WRF model and hourly PM<sub>2.5</sub> concentrations simulated by CMAQ. Among the meteorological parameters,  
 306 wind speed is slightly over predicted with the NMB value of 28%, while temperature, relative humidity and pressure  
 307 all have IOA values greater than 0.9. Figure 3 compares the simulated and observed PM<sub>2.5</sub> concentrations at the  
 308 Shanxi supersite. In general, model predicted data are lower than the observed data with the NMB value of -22% to  
 309 -30%, the NME value of 45% to 47% and the IOA value of 0.67 to 0.70 (Table 2). These underestimations may be  
 310 due to three reasons: Firstly, winter underestimation of PM<sub>2.5</sub> (especially SOA) is a common issue with CMAQ or  
 311 CAMx simulations over China (Hu et al., 2017; Li et al., 2016), which can be explained by a lack of model calculated  
 312 oxidants or missing reactions (Kasibhatla et al., 1997) of SOA formation pathways (Appel et al., 2008; Foley et al.,  
 313 2010). Secondly, uncertainty still exists in the regional emission inventory, including the basic emissions inventory  
 314 and the control scenarios. Thirdly, the wind speed is slightly overestimated over the region, with NMB and NME  
 315 of 28% and 33%, causing fast dispersion of air pollutants. Overall, these statistics for both the meteorological  
 316 parameters and simulated PM<sub>2.5</sub> are generally consistent with the results in other published modelling studies (Zheng  
 317 et al., 2015; Wang et al., 2014; Zhang et al., 2011; Fu et al., 2016; Li et al., 2015b; Li et al., 2015a), which suggests  
 318 that the simulation performance is acceptable.

319 Table 2 Statistics of simulation verification for meteorological parameters and hourly PM<sub>2.5</sub> concentration

Statistical indexes	Wind speed	Temperature	Relative humidity	Air pressure	CAMx-PM <sub>2.5</sub>	CMAQ-PM <sub>2.5</sub>
NMB	28%	3%	-9%	0%	-30%	-22%
NME	33%	14%	12%	0%	45%	47%
IOA	0.81	0.97	0.93	1.00	0.67	0.70

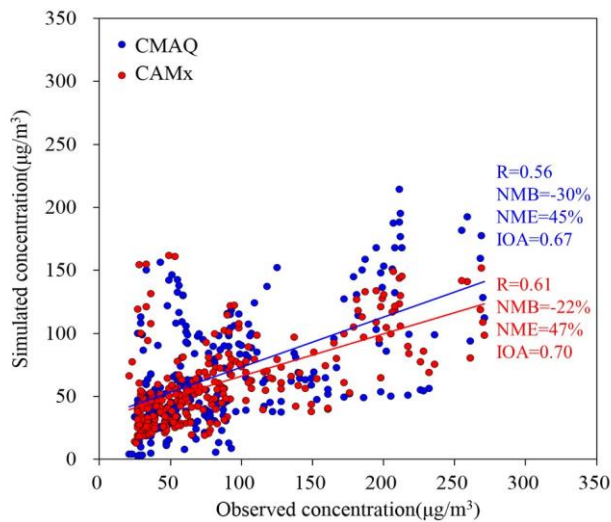


Fig. 3 Scatter plot of the simulated and observed PM<sub>2.5</sub> at the Shanxi supersite

### 2.3.3 Method for quantifying the effectiveness of a control

Quantifying the PM<sub>2.5</sub> reduction in response to emission reductions was done using the so called Brute Force Method (BFM) (Burr and Zhang, 2011), where a baseline scenario was simulated using unadjusted emissions (i.e., those emissions that would have occurred in absence of the Action Plan) and a campaign scenario was modelled based on the emission controls outlined in the Action Plan. In both cases, the same meteorology and chemical boundary conditions were utilized to drive the photochemical model simulations. Through a comparative analysis of the scenarios, a relative improvement factor (RF) for a given atmospheric pollutant, resulting from emission controls, can be calculated and combined with ground based observations to assess the improvement in air quality associated with those emission controls.

$$RF = (C_b - C_s) / C_b \quad (6)$$

$$C_d = C_o \cdot RF \quad (7)$$

where  $C_b$  is the simulated pollutant concentration in the baseline scenario ( $\mu\text{g}/\text{m}^3$ ),  $C_s$  is the pollutant concentration in the campaign scenario ( $\mu\text{g}/\text{m}^3$ ),  $C_o$  denotes the actual observed concentration at the site ( $\mu\text{g}/\text{m}^3$ ) and  $C_d$  is the concentration improvement caused by the control measures ( $\mu\text{g}/\text{m}^3$ ). Utilizing models in a relative sense to assess the efficiency of emission controls on air quality is common practice in regulatory modelling, with the assumption that there may be biases in the absolute concentrations simulated by a modelling system, but that the relative response of that system will reflect the response observed in the atmosphere (US EPA, 2014).

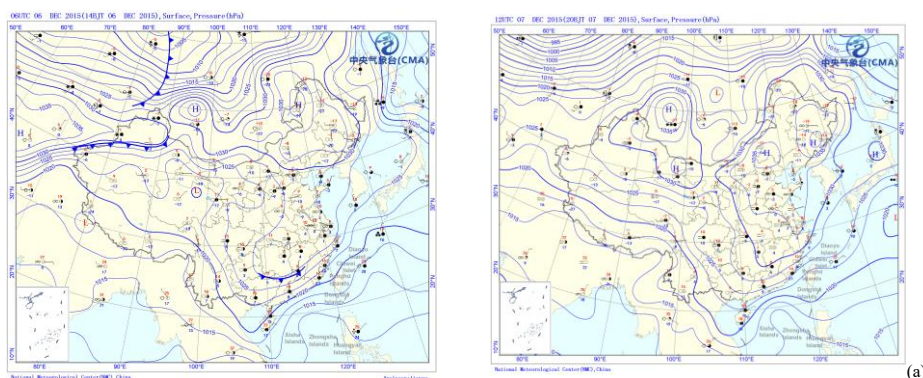
## 3 Results and discussion

340 **3.1 Photochemical transformation changes of air pollutants during the campaign**

341 Ground observational data show that from December 1 to December 23, Jiaxing City experienced four distinct  
342 physical and chemical processes that contributed to the observed pollution levels at different periods. For each of  
343 these processes, this study utilized the integrated emission-measurement-modeling method to analyze the evolution  
344 of air quality from several aspects, including the backward air flow trajectory, potential contribution source areas,  
345 meteorological conditions and the variation of PM<sub>2.5</sub> concentration.

346 **3.1.1 Pollution process before the campaign with local emission accumulation as the main contributor**

347 The first time period of interest was from December 6 to December 8. Analysis about the potential source  
348 contribution areas resulting from PSCF modelling suggests that the polluted air mass primarily originated from the  
349 northwest and northerly airstreams, passing Shandong, the eastern coastal areas of Jiangsu and Shanghai and into  
350 northern Zhejiang, as is shown in Fig. 4. Analysis of the large-scale weather patterns showed that the polluted air  
351 mass occurred in Beijing, Tianjin, Shandong peninsula and northern Jiangsu as a result of cold air with polluted air  
352 mass transported into the region on the morning of December 5. In the southern part of Shandong province, the  
353 PM<sub>2.5</sub> concentration peak appeared on the morning of December 6, while the PM<sub>2.5</sub> concentration peak appeared  
354 around midnight on December 7 at the coastal area of Jiangsu. On December 6, the development of warm and humid  
355 air flow, resulted in increasing ground humidity, which contributed to the growth of secondary fine particles and  
356 the gradual accumulation of polluted air mass in northern Zhejiang and the surrounding areas of Shanghai. On  
357 December 7, affected by the surface high-pressure system, the spread of plume was slow, and the spatial extent of  
358 the plumes in northern Zhejiang expanded. Therefore, during this time period, the pollution was primarily affected  
359 by regional transport and worsened by stagnant local conditions in Jiaxing.



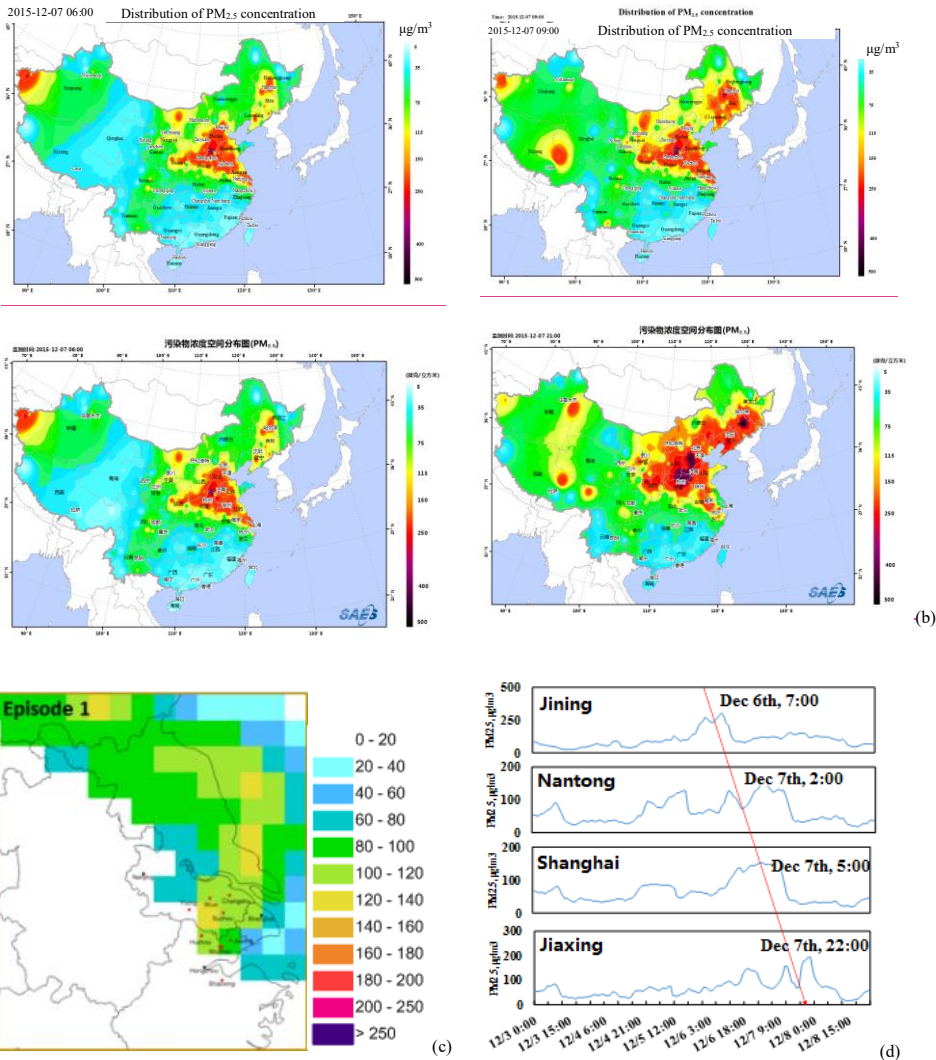


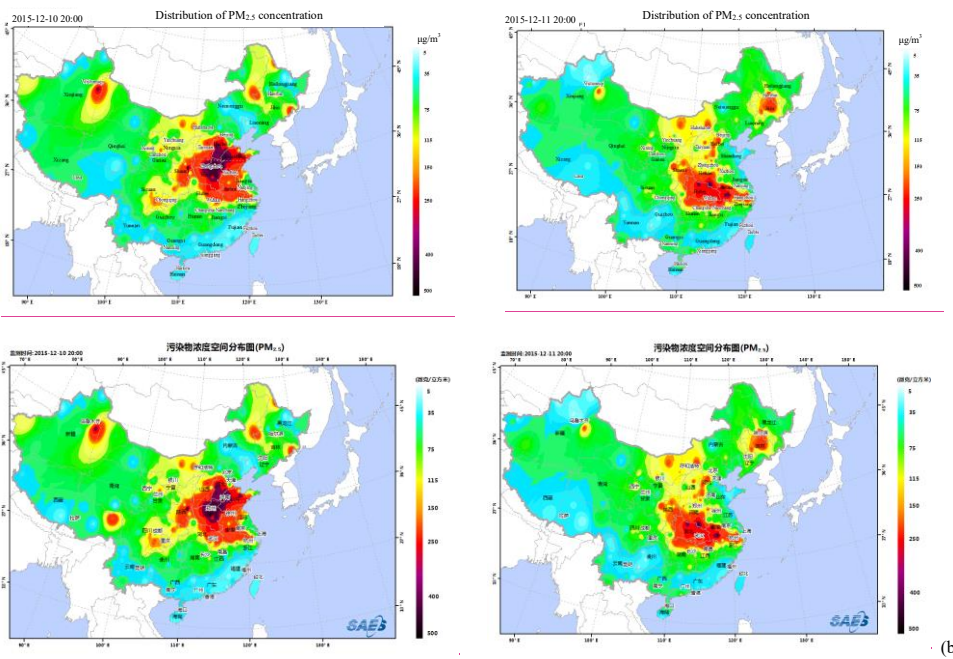
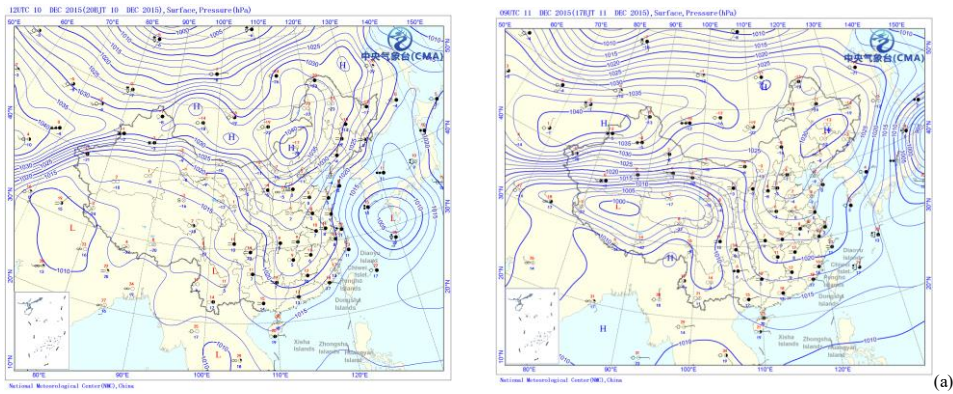
Fig. 4 Analysis of (a) the large-scale weather patterns, (b) distribution of PM<sub>2.5</sub> concentrations, (c) potential source regions, (d) Observed PM<sub>2.5</sub> time series for selected sites during December 6 to December 8, 2015

### 3.1.2 Pollution process during the campaign with the southward motion of the weak cold air

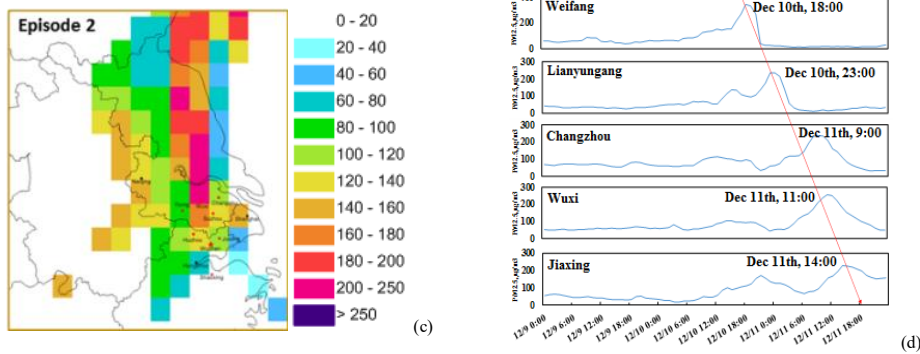
The second time period of interest was from December 10 to December 11. Analysis about potential source contribution areas suggests that the polluted air mass mainly came from northern regions, passing from south-eastern Shandong peninsula and central-eastern Jiangsu to northern Zhejiang. From the large-scale weather pattern, the diffusion of weak cold air on December 10 gradually transported the polluted air mass in the upper reaches of the region to the YRD region. The pollution peaked in areas such as Lianyungang in northern Jiangsu on the evening



368 of December 10. On December 11, the PM<sub>2.5</sub> concentration peak appeared in central and southern Jiangsu as a result  
 369 of northern weak air flow. The plume was further transported into Zhejiang province with the expansion in  
 370 influenced areas as is shown in Figure 5. Therefore, the pollution process was mainly affected by the transport of  
 371 polluted air mass caused by the southward motion of cold air.







372 Fig. 5 Analysis of (a) the large-scale weather patterns, (b) distribution of PM<sub>2.5</sub> concentrations, (c) potential regional sources, (d)  
 373 Observed PM<sub>2.5</sub> time series for select sites during December 10 to December 11, 2015

374 **3.1.2 Heavy pollution process during the campaign with the transit and transport of strong cold air**

375 The third period of interest was from December 13 to the early hours of December 16. Analysis of the potential  
 376 source contribution areas suggests that the polluted air mass mainly came from the northwest direction, passing  
 377 through south-eastern Shanxi, western Shandong, eastern Anhui and western Jiangsu to Zhejiang province. On  
 378 December 14, affected by the cold air transport in the north, northern plumes hit Hebei, Henan and Anhui provinces,  
 379 with the highest degree of pollution on the 14th. On December 15, the further spread of cold air caused the transport  
 380 of plumes into Jiangsu and Zhejiang. The northern part of Zhejiang province was in the centre of pollution on the  
 381 15th, which worsened the pollution and expanded the scope of pollution, as is shown in Figure 6. On December 16,  
 382 under the control of the high-pressure system in northern Zhejiang, the air mass gradually moved eastward and the  
 383 air quality improved in the morning. Therefore, for this time period, large-scale transport was the main factor leading  
 384 to the increase in pollutant levels.

385  
 386  
 387  
 388  
 389

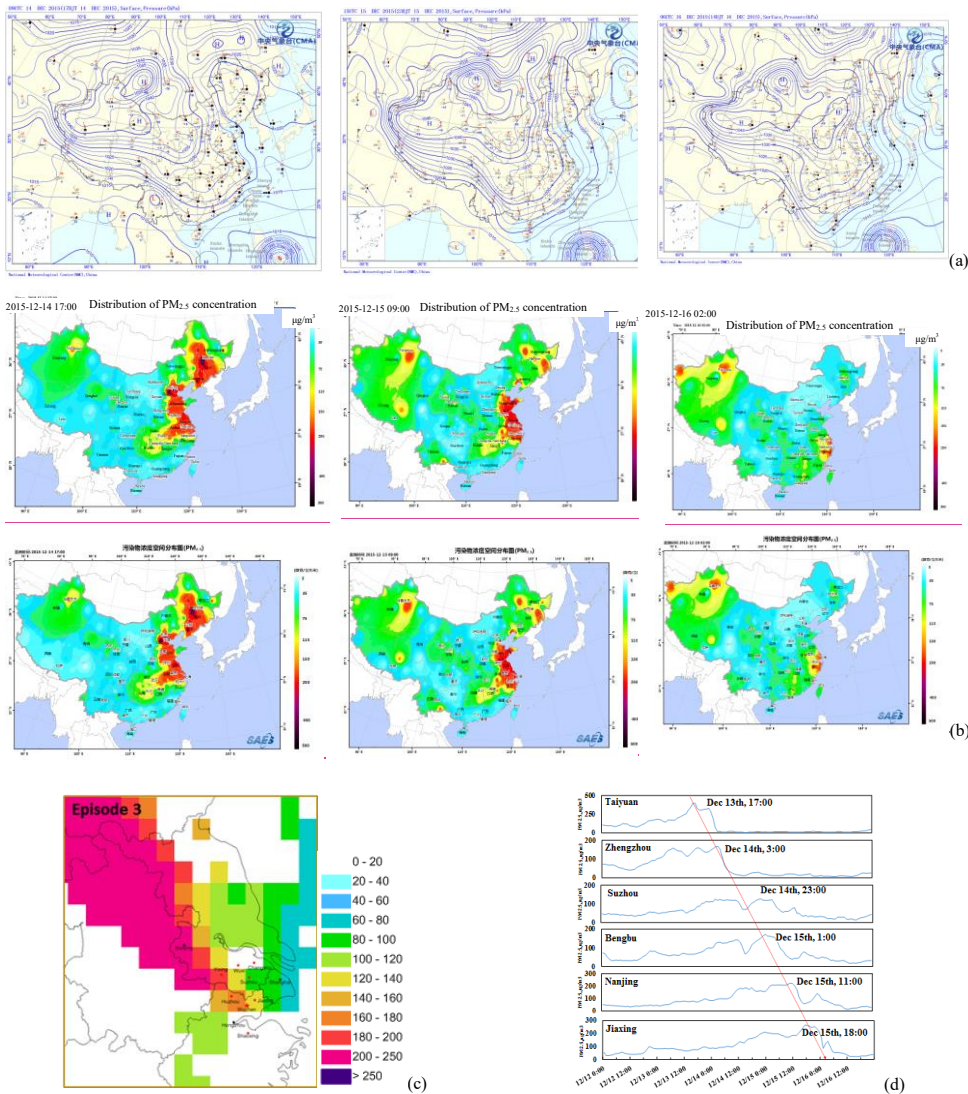


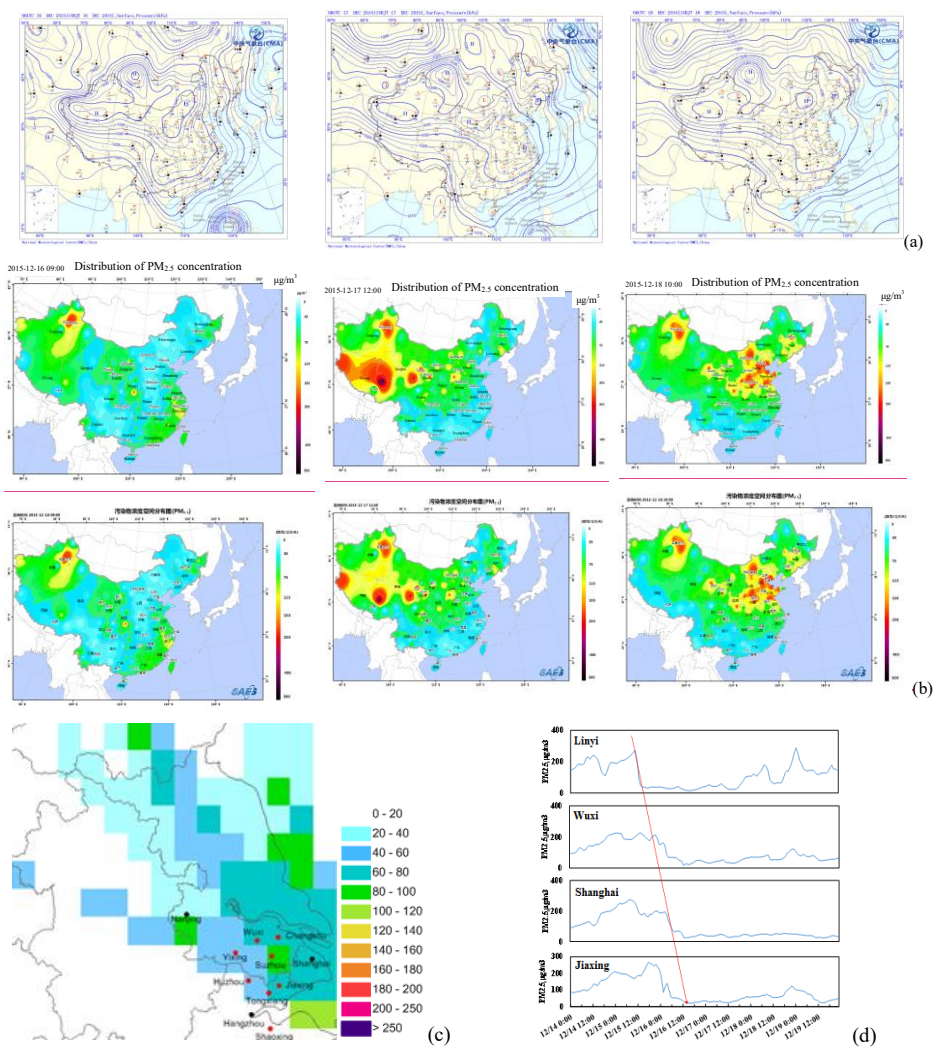
Fig. 6 Analysis of (a) the large-scale weather patterns, (b) distribution of PM<sub>2.5</sub> concentrations, (c) potential regional sources, (d) Observed PM<sub>2.5</sub> time series for select sites during December 14 to December 16, 2015

### 3.1.3 Pollution removal process caused by clean cold air during the conference

During the conference from December 16 to December 18, weather was affected by the large-scale southward transport of cold dry air in northern Zhejiang, resulting in lower temperature and relative humidity, as well as a significant improvement in the air quality. On the 17th and the 18th, under the control of a high pressure system in northern Zhejiang, the sea level pressure increased, the humidity was lower and the wind speed was reduced. Because of the emission reduction effect of the control measures, the pollutant accumulation rate was likely slowed

398 down and the air quality in northern Zhejiang was good overall. From the analysis of potential sources, PM<sub>2.5</sub>  
 399 concentrations in Shandong, Jiangsu and Shanghai were significantly reduced. The PM<sub>2.5</sub> concentration during the  
 400 conference was mainly controlled by local emissions, as is shown in Figure 7.

401

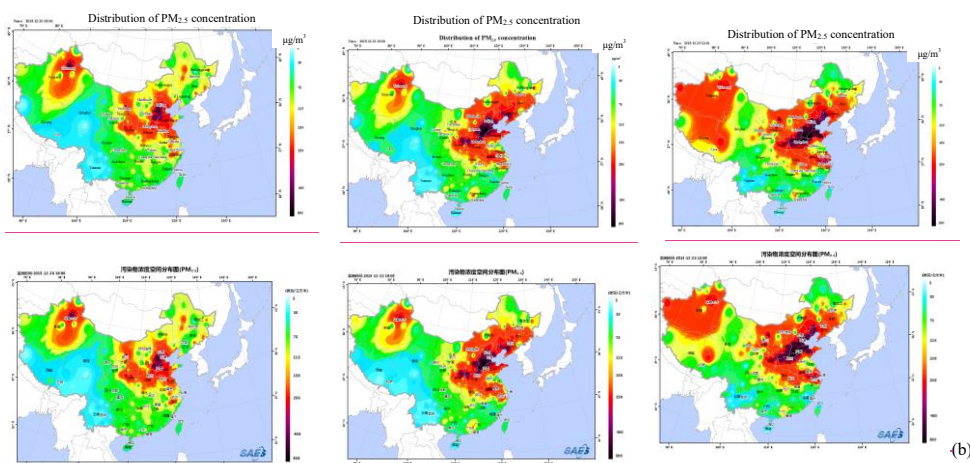
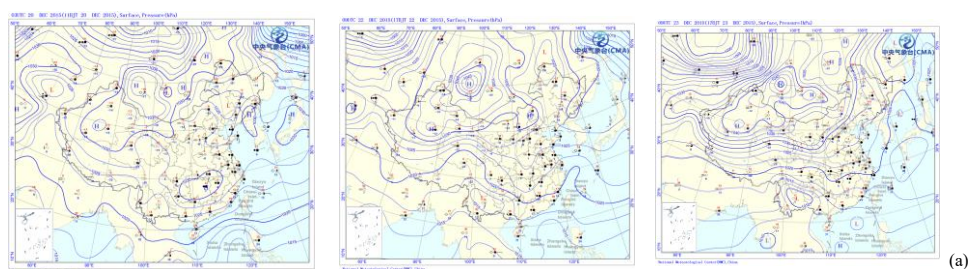


402 Fig. 7 Analysis of (a) the large-scale weather patterns, (b) distribution of PM<sub>2.5</sub> concentrations, (c) potential regional sources, (d)  
 403 Observed PM<sub>2.5</sub> time series for select sites during December 16 to December 18, 2015

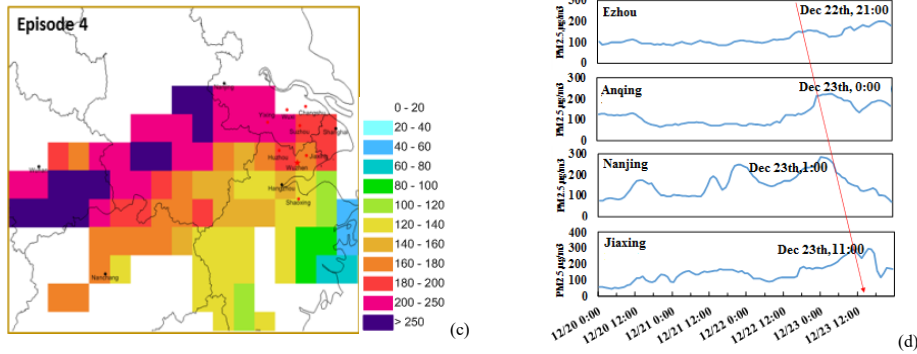
404 **3.1.4 Pollution process after the campaign with local emission accumulation as the main contributor**

405 The fourth period of interest was from December 20 to December 23. Analysis of the potential source  
 406 contribution areas suggests that the polluted air mass mainly came from the southwest direction, passing through

407 southern Hubei, southern Anhui and south-western Jiangsu to northern Zhejiang. On December 20, controlled by a  
 408 stagnant air mass, Zhejiang province has a relatively low near-surface wind speed and little dispersion, resulting in  
 409 the accumulation of local pollutants. On December 21, northern Zhejiang was located in the centre of a high pressure  
 410 system with conditions conducive to little mixing, and therefore polluted air mass occurred in some areas in northern  
 411 Zhejiang. On December 22, affected by the warm and humid southwest air flow, Zhejiang had experienced some  
 412 precipitation but the pollution in northern Zhejiang was not improved due to deep polluted air masses. In Hubei and  
 413 Anhui located in the southwest of Jiaxing City, high pollution levels appeared from the evening of December 22 to  
 414 the early hours of December 23, as is shown in Figure 8. On December 23, the further expansion of polluted air  
 415 masses resulted in serious pollution in Jiangsu and northern Zhejiang. In general, under these heavily polluted  
 416 conditions, the local accumulation of pollutants was mainly caused by stagnant conditions with little dispersion and  
 417 transport within southwest air stream.







418 Fig. 8 Analysis of (a) the large-scale weather patterns, (b) distribution of PM<sub>2.5</sub> concentrations, (c) potential regional sources, (d)  
 419 Observed PM<sub>2.5</sub> time series for select sites during December 20 to December 23

420 **3.2 Air quality changes under the same meteorological conditions before and after the campaign**

421 **3.2.1 Air quality changes under static meteorological conditions before and during the campaign**

422 During the air pollution control campaign for the conference, air quality in Jiaxing City fluctuated greatly due  
 423 to the frequent southward motion of cold air from the north. Under static weather conditions, sources of atmospheric  
 424 pollution mainly came from the accumulation of polluted air masses from local sources and sources in neighbouring  
 425 areas. Therefore, in order to eliminate the influence of the transport process of the air mass, this study compared the  
 426 air quality status before, during and after the campaign in Jiaxing City under stagnant weather conditions (wind  
 427 speed less than 1m/s) and assessed the impact of control measures on ambient air quality in Jiaxing based on air  
 428 quality observation data.

429 Figure 9 shows the concentration levels of criteria pollutants including SO<sub>2</sub>, NO, CO, NO<sub>2</sub> and PM<sub>2.5</sub> in Jiaxing  
 430 City before (December 1-7), during (December 8-19) and after the regulation (December 19-31) under stagnant  
 431 weather conditions. It can be seen that pollutant concentrations during the campaign were less than those before the  
 432 campaign, in which SO<sub>2</sub> had the most significant decline of 40.1%, NO<sub>x</sub>, CO, PM<sub>2.5</sub> and PM<sub>10</sub> declined 8.0%, 2.6%,  
 433 12.5% and 16.3%, respectively, indicating that control measures have significantly improved the air quality in  
 434 Jiaxing City, especially with respect to SO<sub>2</sub> and PM<sub>10</sub>.

435 After the campaign, all the pollutant concentrations rebounded sharply. SO<sub>2</sub>, NO, NO<sub>2</sub>, CO, PM<sub>2.5</sub>, PM<sub>10</sub>  
 436 increased 8.3%, 15.4%, 10.3%, 31.8%, 32.2% and 28.6%, respectively. Concentrations of some pollutants were  
 437 even higher than those before the campaign, which suggests that the emission intensity of the sources had  
 438 significantly increased after the campaign.

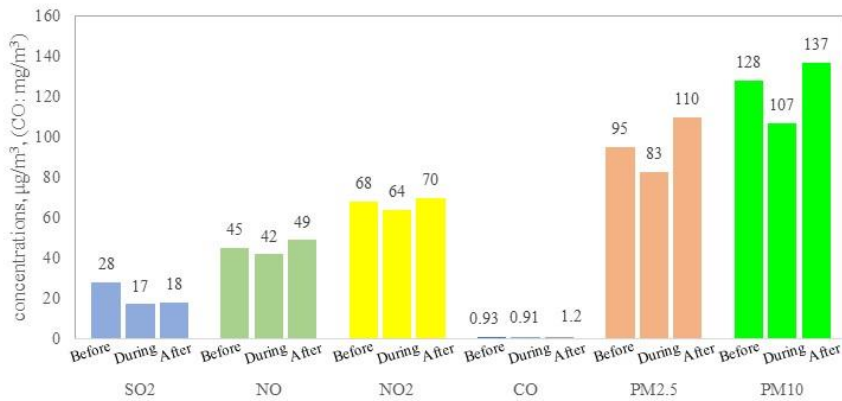


Fig. 9 Comparison between air pollutant concentrations at Shanxi station before, during, and after the campaign under stagnant meteorological conditions

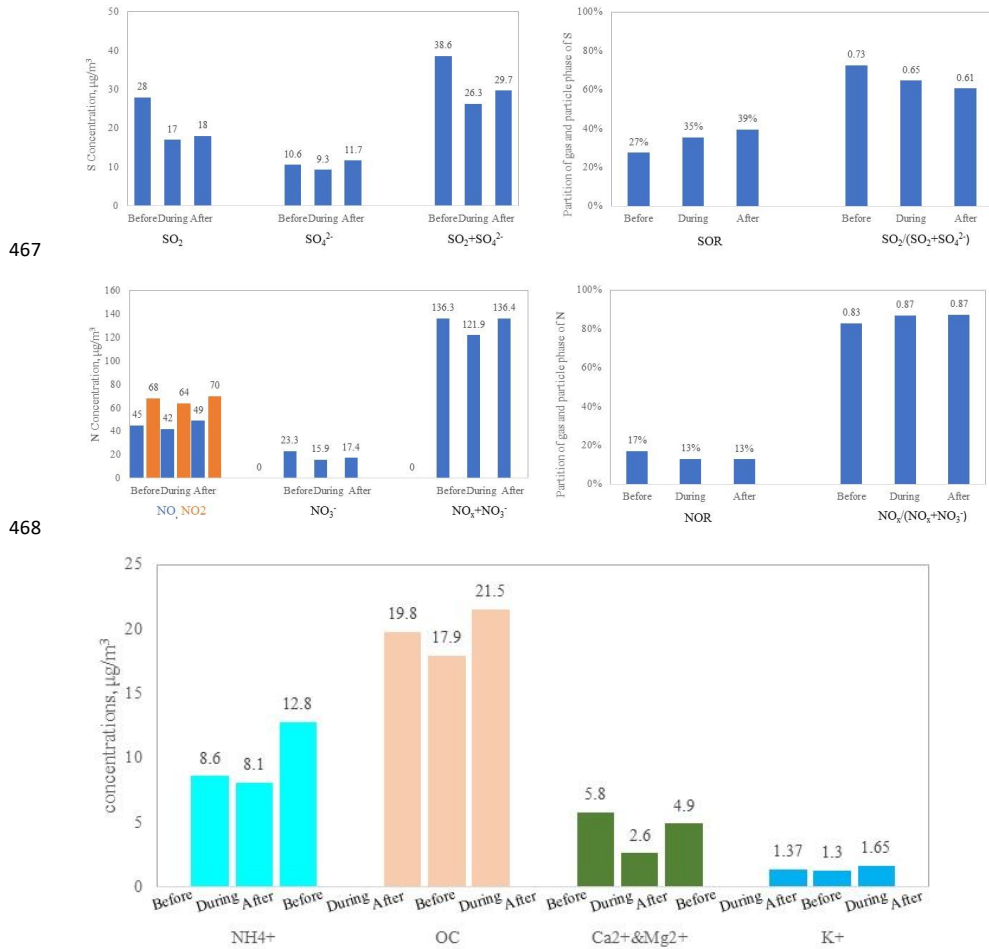
There are also some differences in concentrations of major chemical components of PM<sub>2.5</sub> in Jiaying City before (December 1-7), during (December 8-19) and after the campaign (December 19-31) under static weather conditions, as shown in Figure 9. The concentrations of major chemical components of PM<sub>2.5</sub> during the campaign were less than those before the campaign, which is consistent with the conclusion about changes in criteria pollutant concentrations. On average, SO<sub>4</sub><sup>2-</sup>, NH<sub>4</sub><sup>+</sup>, NO<sub>3</sub><sup>-</sup>, OC, mineral soluble irons (Ca<sup>2+</sup> and Mg<sup>2+</sup>) and K<sup>+</sup> declined 11.8%, 5.1%, 32.1%, 9.8%, 56.8% and 5.1%, respectively. Comparisons between the distribution of PM<sub>2.5</sub> chemical components before and during the campaign under static conditions suggest that Ca<sup>2+</sup> and Mg<sup>2+</sup> decreased most significantly during the control period, which indicates that the suspension of construction operations which result in dust emissions and the rising frequency of rinsing and cleaning paved roads, significantly reduced dust emissions. During the campaign, NO<sub>3</sub><sup>-</sup> significantly decreased, indicating that vehicle control measures successfully reduced NO<sub>x</sub> emissions and subsequently the formation of inorganic aerosols. The significant decrease in SO<sub>4</sub><sup>2-</sup> also shows that restricting or suspending the operation of coal-burning power plants and industries in local and neighbouring cities played a very positive role.

Both the chemical compositions of PM<sub>2.5</sub> and chemical processes associated with PM<sub>2.5</sub> production change. The chemistry also changes if we compare observed data during and after the regulation. As is shown from figure 10, the SO<sub>2</sub> concentrations after control is a little bit higher than during control (+5.9%). However, the SO<sub>4</sub><sup>2-</sup> after control is much higher than during control (25.8%). This is probably due to two reasons: firstly, SO<sub>2</sub> emissions and primary sulfate emissions increased after the control measures were terminated; secondly, previous studies have reported that increased NO<sub>x</sub> emissions could accelerate the formation of secondary sulfate (Cheng et al., 2016). This can be clearly seen from the SOR. A different trend is observed for NO<sub>2</sub> and NO<sub>3</sub><sup>-</sup>, with the NO<sub>2</sub> concentrations

设置了格式: 下标

设置了格式: 下标

462 after control being much higher than during control (+9.4%), while the increase of  $\text{NO}_3^-$  (+9.45%) is about the same.  
 463 Sulfate originates from both primary emissions and secondary formation, but nitrate is mostly secondary. The NOR  
 464 during and after regulation is about the same and most of the N is in the gas phase as indicated by  $\text{NO}_x/(\text{NO}_x+\text{NO}_3^-)$   
 465 (0.87). Therefore, the increase of  $\text{NO}_3^-$  is smaller than  $\text{SO}_4^{2-}$ . The  $\text{PM}_{2.5}$  concentration after control sharply  
 466 rebounded by 31.8%, indicating that both primary emissions and secondary formation are activated.



469 Fig. 10 Comparison between  $\text{PM}_{2.5}$  chemical components at Shanxi station before and after the campaign under static meteorological  
 470 conditions  
 471

472 **3.2.2 Air quality changes under the same air mass trajectory before and during the campaign**

473 In order to distinguish the impact of meteorological conditions on air quality in Jiaying City and better analyze  
 474 the effects of control measures on air quality during the conference, this study has combined meteorological

475 conditions with backward air flow trajectory analysis and carried out a comparative study by selecting a relatively  
 476 similar pollution period before and during the campaign. The first period occurred before the campaign from 12:00  
 477 December 2 to 20:00 December 4, while the second period occurred during the campaign from 9:00 December 16  
 478 to 5:00 December 18. Both of these periods were relatively unaffected by long-range transport of plumes into the  
 479 study area, and have similar backward airflow trajectories and meteorological conditions. Table 3 and Figure 11  
 480 compare average mass concentrations of pollutants (SO<sub>2</sub>, NO<sub>x</sub>, PM<sub>2.5</sub> and PM<sub>10</sub>) during these two periods. As can  
 481 be seen from the figure, SO<sub>2</sub>, PM<sub>2.5</sub> and PM<sub>10</sub> decreased during the campaign by roughly 46%, 13% and 27%,  
 482 respectively, while NO<sub>x</sub> exhibited only a small decrease. This shows that without the impact of long-range transport,  
 483 emission reduction measures carried out by local and surrounding cities play a significant role in defining the air  
 484 quality in Jiaxing.

485  
 486 **Table 3 Concentrations of major pollutants under similar meteorological conditions before and during the campaign**

Period	Time	Wind speed m/s	Wind direction °	Relative humidity %	Temperature °C	Pressure hPa	Visibility km	SO <sub>2</sub> μg/m <sup>3</sup>	NO <sub>2</sub> μg/m <sup>3</sup>	PM <sub>10</sub> μg/m <sup>3</sup>	PM <sub>2.5</sub> μg/m <sup>3</sup>
Before the campaign	12.2 12:00- 12.4 20:00	3.1	268.0	59.2	8.2	102.6	22.8	39.1	44.4	89.5	49.4
During the campaign	12.16 9:00- 12.18 5:00	3.4	247.5	53.0	2.6	103.2	32.1	22.4	39.3	65.3	42.8



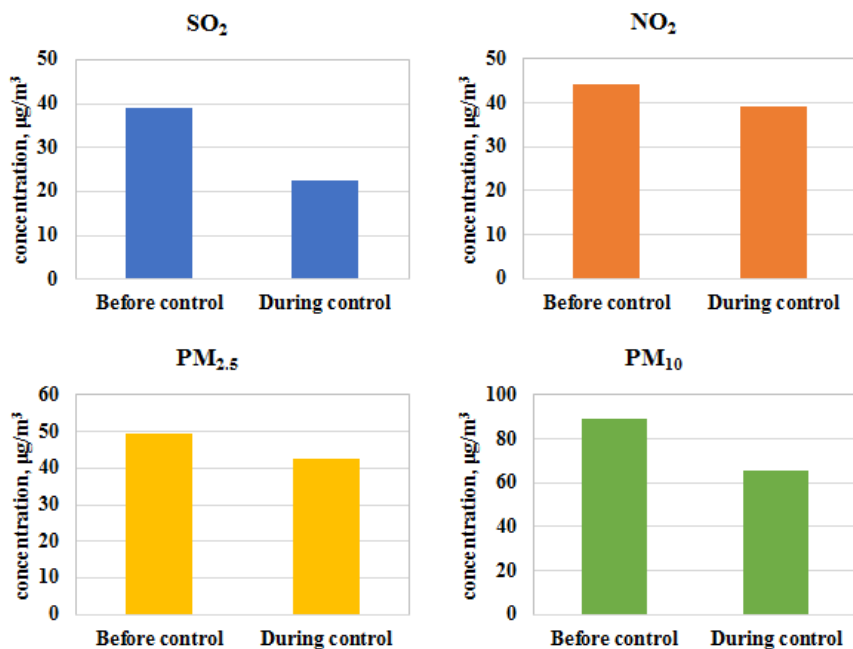


Fig. 11 Comparison between concentrations of major air pollutants in Jiaxing before and after the campaign under same meteorological conditions

487  
488  
489  
490

491 There were two regional pollution episodes that occurred during the campaign. The first was on December 10-  
492 12 caused by the southward motion of northern weak cold air. Polluted air masses from south-eastern Shandong  
493 peninsula passed through central eastern Jiangsu and into northern Zhejiang, affecting the air quality in Jiaxing.  
494 During this period, the average daily PM<sub>2.5</sub> concentration in Jiaxing was 145.7 µg/m<sup>3</sup>, higher than the regional  
495 average, and its major chemical components were nitrate (31%), sulphate (18%), ammonium (13%) and organic  
496 carbon (13%), with obvious regional secondary pollution characteristics.

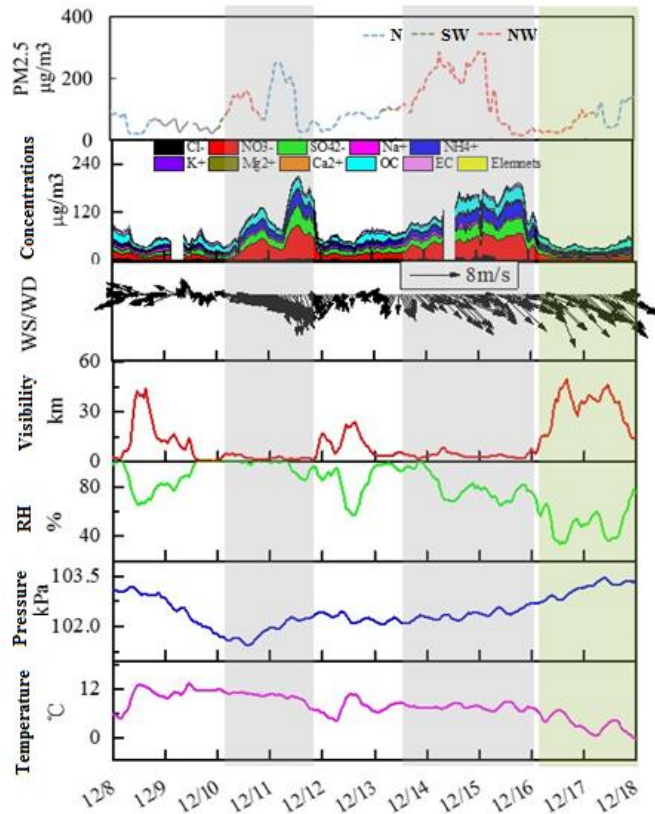


Fig.12 Changes in air quality and meteorological parameters in Jiaxing City during the campaign

497  
498

499 The second episode occurred from December 14-15, and was caused by the transit of northwesterly strong cold  
500 air. Polluted air masses came from the northwest direction, moved rapidly to the southeast, passed through Shanxi,  
501 Hebei, west Shandong, east Anhui and west Jiangsu and ultimately into Zhejiang province. The air masses left  
502 China through south-eastern Zhejiang on the early morning of the 16th. The YRD region was strongly affected by  
503 the transport of the polluted air mass, with heavy polluted air masses appearing and lasting for about one day over  
504 the YRD region from north to south. PM<sub>2.5</sub> peaked in Jiaxing on the 15th with a daily average of 201.6 µg/m<sup>3</sup>. The  
505 main chemical components of PM<sub>2.5</sub> during the episode were nitrate (25%), sulphate (14%), ammonium (12%) and  
506 organic carbon (13%), which is consistent with an aged air mass as well as regional secondary pollution  
507 characteristics.

508 The regional linkage was initiated from December 16 to December 18, combined with favourable mixing  
509 conditions brought by the cold front. The overall air quality in the YRD region during this time period was good,  
510 with an average daily PM<sub>2.5</sub> concentration in Jiaxing of 45 µg/m<sup>3</sup>. The major chemical components during this

511 cleaner period were organic carbon (26%), nitrate (16%), ammonium (12%), sulphate (9%) and other components  
512 (37%), with some newly formed particles and no obvious regional transport, suggesting that air pollutants were  
513 mainly derived from local emissions.

### 514 3.3 Emissions reduction estimation during the campaign

515 The air quality assurance campaign for the 2<sup>nd</sup> World Internet Conference was from December 8 to December  
516 18. In order to ensure the air quality during the conference, three provinces and Shanghai municipality in the YRD  
517 region carried out joint control measures. Based on the implementation of control measures in all areas during the  
518 conference and whether each area had effectively implemented control measures during December 8-18, regional  
519 emission reductions have been assessed. It is estimated that emission reductions of SO<sub>2</sub>, NO<sub>x</sub>, PM<sub>2.5</sub> and VOCs  
520 caused by production restriction in regional industrial enterprises are 2867.8 tons, 3064.7 tons, 2165.5 tons and  
521 5055.4 tons, respectively. Emission reductions of various pollutants caused by the restrictions on motor vehicle  
522 traffic are estimated to be 4.7 tons of SO<sub>2</sub>, 326.9 tons of NO<sub>x</sub>, 36.1 tons of PM<sub>2.5</sub> and 452.5 tons of VOCs. Emission  
523 reduction of PM<sub>2.5</sub> caused by dust control was estimated to be 266.0 tons. Therefore, it can be seen that emission  
524 reductions mainly come from industrial sources, while motor vehicle restrictions contributed greatly to emission  
525 reductions of NO<sub>x</sub> and VOCs, and dust control contributed 10% to emission reductions of PM<sub>2.5</sub>.

526 When looking at specific industries, the power plants contributed most to the emission reductions of SO<sub>2</sub> and  
527 NO<sub>x</sub> at 49.7% and 46.9%, respectively, followed by the chemical industry, building materials industry, steel industry  
528 and petrochemical industry with a total contribution from all four sectors to emission reductions of SO<sub>2</sub> and NO<sub>x</sub> of  
529 42.0% and 47.2%, respectively. For PM<sub>2.5</sub>, the building materials industry contributed the most at 62.0%, followed  
530 by steel and processing industry, power industry and non-ferrous smelting and process industry with a contribution  
531 of 14.3%, 13.1% and 8.1%, respectively. For VOCs, the emission reduction sectors are mainly chemical,  
532 petrochemical and machinery manufacturing sectors with a total contribution of 65.7% and individual contributions  
533 of 25.1%, 23.2% and 17.4%, respectively. In addition, metal products processing, building materials and steel and  
534 processing sectors also contributed significantly to emission reductions of 13.4%, 8.0% and 6.5%, respectively.

535 In terms of the regional distribution of emission reductions, Jiaxing, Hangzhou, Suzhou and Shaoxing have the  
536 largest contribution of around 80%. These four cities contribute 87% to the total emission reduction of PM<sub>2.5</sub>.

537 Combing all control measures, total emission reductions of SO<sub>2</sub>, NO<sub>x</sub>, PM<sub>2.5</sub> and VOCs are estimated to be  
538 2872.5 tons, 3391.6 tons, 2467.6 tons and 5507.9 tons, respectively, which accounts for 10%, 9%, 10% and 11%,  
539 respectively, of the total urban emissions. It is worth mentioning that if we consider the emergency emission  
540 reduction measures for heavy pollution during the campaign, the amount of emission reduction for all pollutants

541 and the proportion of their emission reductions would be even larger. Table 4 shows the percentage and the amount  
 542 of emission reductions for pollutants under various control measures.

543  
 544 Table 4 Emission reduction estimations for various control measures

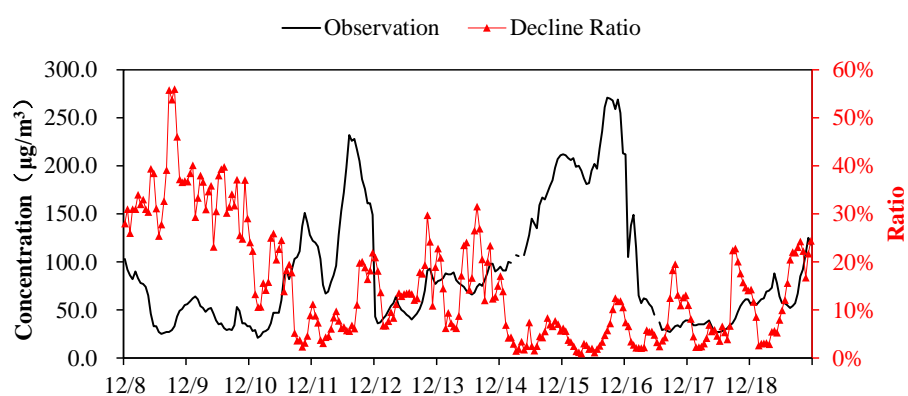
Province	City	Sector	Amount of emission reduction (tons)				Percentage of reduction			
			SO <sub>2</sub>	NO <sub>x</sub>	PM <sub>2.5</sub>	VOCs	SO <sub>2</sub>	NO <sub>x</sub>	PM <sub>2.5</sub>	VOCs
Zhejiang	Jiaxing		925.6	709.5	462.3	1872.7	56%	58%	64%	80%
	Huzhou		414.8	585.6	602.5	514.0	46%	37%	47%	53%
	Hangzhou		657.2	654.1	476.2	1043.2	36%	42%	59%	33%
	Ningbo	Industries	59.1	65.3	107.5	84.0	32%	30%	37%	33%
	Shaoxing	and enterprises	365.9	414.8	403.9	678.7	34%	38%	62%	31%
Shanghai	Shanghai		253.6	368.7	83.6	796.1	9%	7%	6%	8%
Jiangsu	Suzhou		89.4	34.9	10.2	11.4	3%	1%	1%	1%
	Wuxi		94.4	163.0	10.2	55.3	12%	10%	1%	5%
Anhui	Xuancheng		7.8	68.8	9.1	0.0	15%	42%	28%	0%
	<b>Sub-total</b>		<b>2867.8</b>	<b>3064.7</b>	<b>2165.5</b>	<b>5055.4</b>	<b>23%</b>	<b>19%</b>	<b>27%</b>	<b>19%</b>
Zhejiang	Jiaxing	Motor vehicles	2.3	157.7	16.4	211.3	46%	53%	38%	25%
	Huzhou		0.7	48.4	6.2	81.0	23%	24%	19%	12%
	Hangzhou		1.7	120.8	13.5	160.2	8%	15%	20%	20%
	<b>Sub-total</b>		<b>4.7</b>	<b>326.9</b>	<b>36.1</b>	<b>452.5</b>	<b>15%</b>	<b>25%</b>	<b>25%</b>	<b>19%</b>
Zhejiang	Jiaxing	Dust control	/	/	119.5	/	/	/	100%	/
	Huzhou		/	/	11.1	/	/	/	10%	/
	Hangzhou		/	/	26.6	/	/	/	10%	/
	Ningbo		/	/	28.8	/	/	/	5%	/
	Shaoxing		/	/	5.8	/	/	/	5%	/
Shanghai	Shanghai		/	/	69.3	/	/	/	6%	/
Jiangsu	Suzhou		/	/	2.7	/	/	/	1%	/
	Wuxi		/	/	1.8	/	/	/	1%	/
Anhui	Xuancheng		/	/	0.4	/	/	/	1%	/
	<b>Sub-total</b>		/	/	<b>266.0</b>	/	/	/	<b>9%</b>	/
	<b>In total</b>		<b>2872.5</b>	<b>3391.6</b>	<b>2467.6</b>	<b>5507.9</b>	<b>10%</b>	<b>9%</b>	<b>10%</b>	<b>11%</b>

545  
 546 **3.4 Quantitative estimates of the contribution of control measures to air quality improvement**

547 **3.4.1 PM<sub>2.5</sub> concentration improvement in Jiaxing**

548 The WRF-CMAQ air quality model, combined with observations, was used to evaluate the improvement of  
 549 PM<sub>2.5</sub> in Jiaxing due to the emission reductions achieved through the campaign. This analysis utilized two model  
 550 simulations to assess the impact of the emission reductions: 1) a baseline scenario, which utilized an uncontrolled  
 551 emission inventory (i.e., the emissions that would have occurred without the campaign), and 2) an emission  
 552 inventory, which reflects the emission reductions achieved by the campaign. Figure 13 shows the time series of  
 553 PM<sub>2.5</sub> observed concentrations and the percent change in PM<sub>2.5</sub> after the air quality control measures were  
 554 implemented. It can be seen that the PM<sub>2.5</sub> decline ratio in Jiaxing varies with time. The PM<sub>2.5</sub> decline ratio was

555 most significant during December 8-9 with a maximum reduction of 56%. During the campaign from December 8  
 556 to December 18, average  $PM_{2.5}$  concentrations decreased by  $10.5 \mu\text{g}/\text{m}^3$  with an average decrease of 14.4%.  
 557 However, Although there are many control strategies implemented, the effects during 12/14-12/16 are low. As  
 558 described in section 3.1.2, the prevailing wind direction during this period is NW, and Jiaxing experienced a heavy  
 559 pollution process with the transit and transport of strong cold air. Therefore, we can not see obvious effect without  
 560 strong upwind precursor emissions reductions.



561 Fig. 13 Time series of observed  $PM_{2.5}$  and the percentage reduction resulting from the implementation of air quality control measures

562 Figure 14 shows the reduction in daily average  $PM_{2.5}$  concentrations in Jiaxing resulting from the emission  
 563 reductions associated with the Action Plan for Air Quality Control during the World Internet Conference. As can  
 564 be seen from the figure, the improvement in  $PM_{2.5}$  before the conference (December 8 and 9) was relatively  
 565 significant, with a daily average decline of roughly 31% and 35%, respectively, which corresponds to a decrease of  
 566 around  $17 \mu\text{g}/\text{m}^3$ . The reduction in  $PM_{2.5}$  during December 14-15, two of the days with some of the highest observed  
 567  $PM_{2.5}$ , was relatively low at around 6%, while daily average  $PM_{2.5}$  concentrations on those days decreased by around  
 568  $10.0 \mu\text{g}/\text{m}^3$ . The magnitude of emission reductions during those two time periods was basically the same, so it's  
 569 likely that the observed difference in  $PM_{2.5}$  levels was the result of meteorological differences, and in particular,  
 570 enhanced transport of polluted air into Jiaxing from December 14 to 15. Overall, under the influence of regional  
 571 control measures for emission reductions from December 8 to December 18,  $PM_{2.5}$  daily average concentration  
 572 decreased by 5.5%-34.8% with an average of 14.6% or  $10 \mu\text{g}/\text{m}^3$ .  
 573

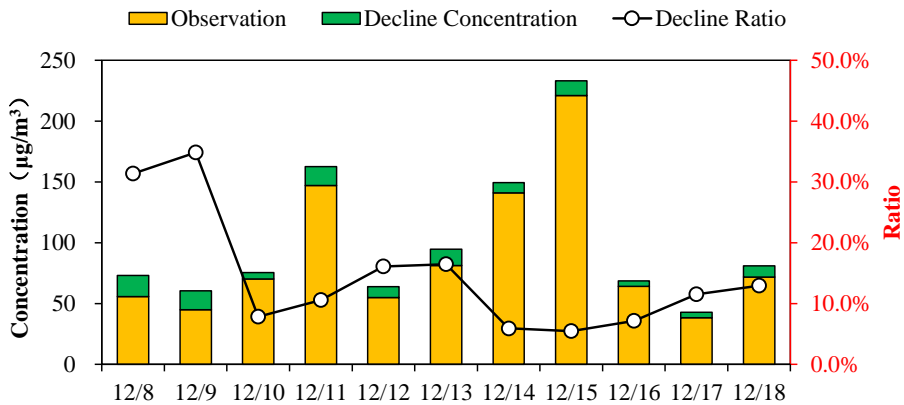


Fig.14 Percentage reduction in PM<sub>2.5</sub> resulting from the control measures

574  
575

576 The decline ratio changes with meteorological conditions even under the same emissions reduction situation,  
577 because meteorological conditions influence dispersion from primary emissions, regional transport and secondary  
578 formation. The magnitude of emission reductions during those two time periods was basically the same, so it is  
579 possible that the observed difference in PM<sub>2.5</sub> levels was the result of meteorological differences. Overall, the  
580 residual PM<sub>2.5</sub> may come from three aspects: (1) although stringent control measures have been implemented, there  
581 are still some precursor emissions in the city, which accumulated and formed secondary particles under favorable  
582 meteorological conditions; (2) enhanced transport under specific meteorological conditions, especially upwind  
583 emissions; (3) in view of the uncertainties of model performance (underestimation of PM<sub>2.5</sub>, especially  
584 underestimation of SOA) described in previous sections, it should be noted that the secondary formation may  
585 probably be underestimated, causing modeled decline ratio lower than observed.

### 586 3.4.2 PM<sub>2.5</sub> concentration improvement across regions

587 Figure 15 shows the spatial distribution of PM<sub>2.5</sub> concentrations in the Yangtze River Delta region from  
588 December 8 to December 18 in the baseline scenario and the campaign scenario. As can be seen from the figure,  
589 southern Jiangsu, Shanghai and northern Zhejiang in the central YRD region had relatively high PM<sub>2.5</sub>  
590 concentrations, which is consistent with the typically more serious pollution levels in autumn and winter in the YRD  
591 region. Under the influence of regional control measures, PM<sub>2.5</sub> average concentrations declined significantly in  
592 Jiaxing, Hangzhou and Huzhou, especially at the junction of these three cities, with a slight improvement in central  
593 southern Zhejiang as well. The average percentage PM<sub>2.5</sub> decline ratio in Jiaxing, Hangzhou and Huzhou was about  
594 6%-20%. Meanwhile, given that the prevailing winds are north-westerly in winter, there was also some  
595 improvement in central and southern Zhejiang.

596  
597  
598  
599

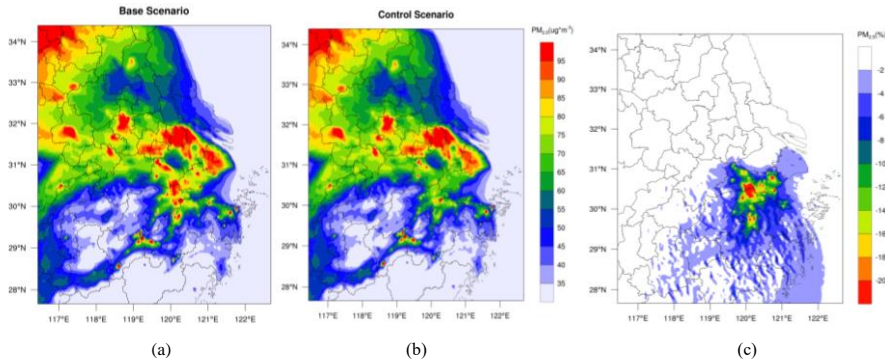


Fig. 15 Spatial distribution of PM<sub>2.5</sub> concentrations in the Yangtze River Delta region under the baseline scenario (a) and the campaign scenario (b), and the percentage reduction in PM<sub>2.5</sub> throughout the YRD region (c)

600 **3.4.3 Regional contributions of PM<sub>2.5</sub> concentration improvement in Jiaxing**

601 Figure 16(a) shows the percentage reduction in PM<sub>2.5</sub> daily average concentrations from December 13 to  
602 December 18 after control measures were implemented in Jiaxing and regionally. The reduction in PM<sub>2.5</sub> was the  
603 results of both local controls, as well as regional controls which reduced pollution in the air masses transported into  
604 Jiaxing. Overall, modelling suggests that the regional controls reduced PM<sub>2.5</sub> levels in Jiaxing between 5.5%-16.5%  
605 (9.9% average), while local control measures contributed 4.5%-14.4%, with an average of 8.8%.

606 Figure 16(b) shows the average contribution of local emissions reductions in Jiaxing and in the YRD region  
607 over the entire campaign (Dec.13-18), as well as the corresponding improvement in PM<sub>2.5</sub> levels in Jiaxing. During  
608 this period, PM<sub>2.5</sub> daily average concentration declined by 4-13 μg/m<sup>3</sup>, while there were differences in the  
609 contribution of regional remission reductions and local emission reductions in Jiaxing during different periods.  
610 Overall, local control measure in Jiaxing had the largest impact on PM<sub>2.5</sub> levels and accounted for 89% of the decline  
611 in PM<sub>2.5</sub>, while regional control measures contributed the remaining 11%.

612  
613

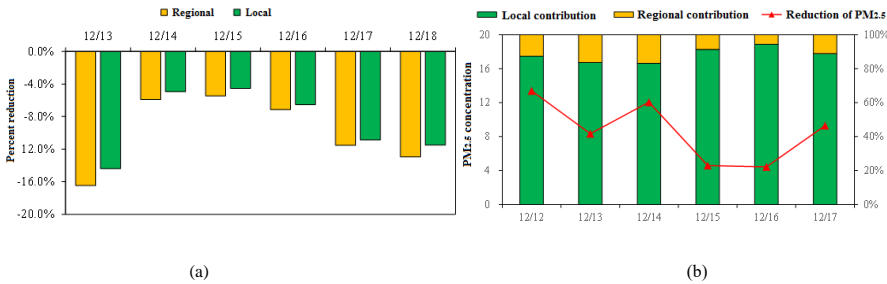


Fig. 16 Percentage reduction in daily average PM<sub>2.5</sub> concentrations from December 13 to December 18 after implementation of the control measures across the region and in Jiaxing (a) and Contribution of local and regional emissions reductions in Jiaxing, and the resulting improvement of daily average PM<sub>2.5</sub> concentrations in Jiaxing (b)

617 **3.5 Optimisation scenario analysis of regional linkage control measures**

618 **3.5.1 Optimization scenario settings**

619 In order to further analyse the optimisation potential of air quality control measures for major events and  
 620 enhance the effectiveness of the control measure scheme design, three control measure optimisation scenarios have  
 621 been set on the basis of the evaluation scenario (Base) after the implementation of air quality control measures  
 622 during the conference. These scenarios include local emission reductions in Jiaxing under stagnant meteorological  
 623 conditions, where local emission accumulation is the main contributor to the pollution process (Sc.1), and the  
 624 emission reduction scenario where transport of polluted air masses into Jiaxing is a major contributor to the PM<sub>2.5</sub>  
 625 levels in Jiaxing. In order to investigate the transport processes further, the latter scenario was further divided into  
 626 a scenario 24 hours in advance (Sc.2) and a scenario 48 hours in advance (Sc.3). Table 5 describes the details of  
 627 each scenario.

628 Table 5 Control measure optimization scenario settings  
 629

Scenario name	Scenario settings	Emission reduction regions	Emission reduction measures	Starting time
Base	Regional emission reduction	All the cities and areas involved in the campaign scheme	All control measures mentioned in the campaign scheme	December 8
Sc.1	Local emission reduction in Jiaxing	Jiaxing	Control measures in Jiaxing mentioned in the campaign scheme	December 8
Sc.2	Emission reduction through transport channels 24 hours in advance	Cities located in the northwest transport channel of Jiaxing	Cut down industrial sources by 30%	December 13
Sc.3	Emission reduction through transport channels 48 hours in advance	Cities located in the northwest transport channel of Jiaxing	Cut down industrial sources by 30%	December 12

630 Figure 17 shows the cities that primarily influence the polluted air masses transported into Jiaxing, where the  
 631 transport channels were determined through backward trajectory analysis. These cities include Huzhou in Zhejiang  
 632 province, Suzhou, Wuxi, Changzhou, Nanjing, Zhenjiang, Huai'an, Suqian and Suzhou in Jiangsu province and  
 633 Suzhou, Huaibei, Bozhou, Bengbu, Chuzhou and Ma'anshan in Anhui province. Each of these cities took measures  
 634 to reduce emissions by limiting production from industry industries by 30%.



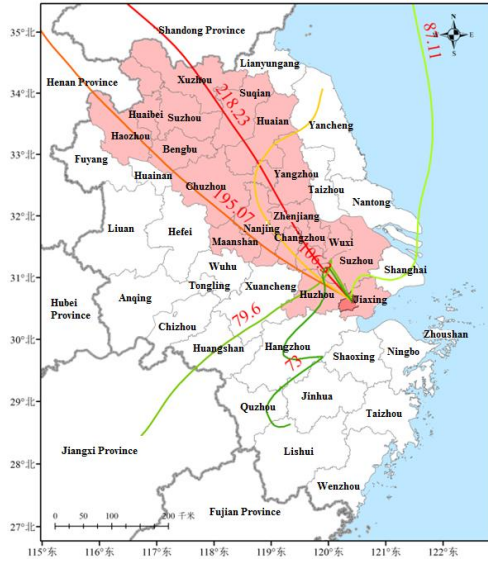


Fig. 17 Cities involved in the transport channel and the emission reduction channel

The WRF-CMAQ modelling system was used to analyse and compare the air quality improvement effect under different pollution process in four scenarios.

### 3.5.2 Analysis of optimization scenario effects

In order to evaluate the effect of the different starting time for the same control measures, and the same starting time for local and regional control measures, we investigated four scenarios. Figure 18 shows the percentage reduction in daily average  $PM_{2.5}$  concentrations in Jiaxing City from December 13 to December 18 under the regional emission reduction scenario, the Jiaxing local emission reduction scenario and the transport channel emission reduction scenario. Overall, there are differences in the distribution of  $PM_{2.5}$  under the different scenarios. The air quality improvement due to the regional emission reductions was higher than that of local emission reductions in Jiaxing, and lower than that of channel emission reductions.

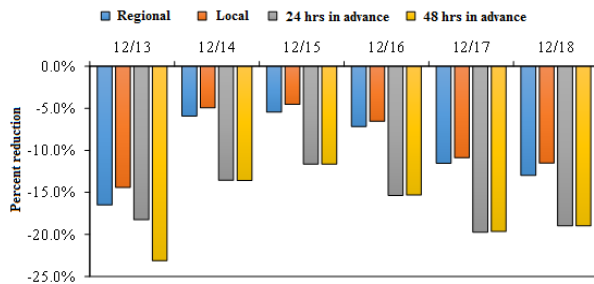


Fig. 18 Decline rates of  $PM_{2.5}$  daily average concentrations in Jiaxing under different scenarios

649 **(1) Effect of local emission reductions in Jiaying**

650 By comparing the effect of local emission reductions in Jiaying (Sce.1) and the effect of regional emission  
651 reductions (Base), we can see that PM<sub>2.5</sub> daily average concentrations in Jiaying declined by around 5.5%-16.5%  
652 under the regional emission reduction plan (regional emission plan including the local emissions control) from  
653 December 13 to December 18 and by around 4.5%-14.4% under the local emission reduction plan. Local emission  
654 reductions in Jiaying contributed 83%-94% to the emission reduction effect. Therefore, local emission reduction in  
655 Jiaying is the key factor in improving the local air quality.

656 Compared with the channel emission reduction scenario 24 hours in advance (11.6%-18.2%), local emission  
657 reductions also contributed more than 50% to the improvement effect on December 13, 17 and 18. Therefore, local  
658 emission reductions contributed most to the air quality improvement effect in Jiaying, indicating that local areas are  
659 still the most important control areas during the campaign.

660 **(2) Effect of emission reductions through transport channels**

661 As mentioned above, during the large-scale transport of heavily polluted air masses into the Yangtze River  
662 Delta region from December 14 to December 15, the PM<sub>2.5</sub> pollution in Jiaying was significantly affected. Under  
663 the local emission reduction scenario (Sce.1) and the regional linkage emission reduction scenario (Base), PM<sub>2.5</sub>  
664 daily average concentrations in Jiaying decline by only 4.5%-5.9%. If a 30% reduction in emissions from industrial  
665 sources in the upwind transport channel is implemented, PM<sub>2.5</sub> daily average concentrations in Jiaying declined by  
666 11.6%-13.6%, while local emission reductions contributed less than 40% to the improvement of PM<sub>2.5</sub>. Therefore,  
667 to reduce PM<sub>2.5</sub> under these large-scale transport conditions, in addition to intensifying local emission reduction  
668 efforts, it is more effective to prevent and control such pollution by adopting emission reductions of industrial  
669 sources over key transport channels, especially for elevated sources.

670 In this study, the main transport channel involved is the northwest transport channel in control areas, which  
671 basically represents the typical winter transport channel in the region. In this study, the main transport channel  
672 involved is the northwest transport channel in control areas, which basically represents the typical winter transport  
673 channel in the region. Air quality improvement due to regional emission reductions was slightly larger than that of  
674 local emission reductions in Jiaying, and smaller than that of channel emission reductions. This suggests that  
675 emissions reduction in the downwind cities does not have much effect on Jiaying's air quality. In contrast, emissions  
676 reduction based on predicted transport pathway in advance are much more effective than local emissions reduction  
677 as well as regional emission reductions. Therefore, a well-designed management plan for the main transport channel  
678 is necessary to ensure optimized air quality improvement in autumn and winter, in addition to reducing local

679 emissions.

### 680 **(3) Effect of the starting time for channel emission reductions**

681 According to the comparisons between the emission reduction scenario 24 hours in advance (Sce.2) and the  
682 emission reduction scenario 48 hours in advance (Sce.3) during the large-scale PM<sub>2.5</sub> transport, we can see that if  
683 we take December 13 as the target and adopt channel emission reductions 48 hours in advance, PM<sub>2.5</sub> daily average  
684 concentrations will decline by 23.1% when compared to the baseline scenario, which is significantly better than the  
685 improvement achieved by the emission reduction scenario 24 hours in advance (18.2%). Therefore, early measures  
686 to reduce emissions will lead to the improvement of air quality.

687 If we focus on the conference period (December 16-18), PM<sub>2.5</sub> daily average concentrations will both decline  
688 by 15.3%-19.7% under the two channel emission reduction scenarios, indicating a close improvement effect.  
689 Therefore, during the pollution process when local emissions are the main contributor, local emission reductions  
690 should be the top priority with no difference between channel reductions 24 hours in advance and 48 hours in  
691 advance. If transport is the main contributor to the pollution, adopting channel reductions 48 hours in advance can  
692 bring about more improvement effect than 24 hours in advance.

## 693 **4 Conclusions**

694 **(1) The effect of restricting production in industrial enterprises is remarkable.** The power industry and  
695 related industrial enterprises in Jiaxing cut down SO<sub>2</sub> and NO<sub>x</sub> emissions by over 50%, while the building materials  
696 industry, smelting industry and other industrial enterprises cut down PM<sub>2.5</sub> emissions by 63%, contributing greatly  
697 to the reduction of primary PM<sub>2.5</sub> concentrations. The petrochemical industry, chemical industry and other related  
698 industrial enterprises cut down VOCs emission by 66% in total, contributing greatly to the reduction of PM<sub>2.5</sub> formed  
699 through the conversion of precursor species. The observation data of PM<sub>2.5</sub> components suggest that the relative  
700 contribution of secondary components dropped significantly during the conference. Production restriction or  
701 suspension for industrial enterprises is the main contributor to emission reductions for various pollutants during the  
702 campaign, which resulted in the largest improvement in air quality.

703 **(2) Motor vehicle pollutant emissions declined significantly.** In Jiaxing, motor vehicle restrictions were fully  
704 implemented during heavy pollution days, temporary traffic control was implemented during certain periods, and  
705 enterprises and institutions had a three-day vacation during the conference. Emission reduction rates for various  
706 pollutants from motor vehicle emissions were around 40%-50%. Motor vehicle emission reduction measures  
707 contributed to the total emission reductions of nitrogen oxides by 18.2%, fine particles by 3.4% and volatile organic  
708 compounds by 10.1%.

709       **(3) The effect of dust control measures is remarkable.** During the conference, most of the construction sites  
710 in Jiaxing were suspended from operation. Increased frequency for road cleaning activities greatly lowered the dust  
711 emissions. Speciation of the measured PM<sub>2.5</sub> suggest that the mass concentration of crust material, decreased by 14%  
712 compared to measurements after the conference. Specially, under static conditions, mineral soluble irons (Ca<sup>2+</sup> and  
713 Mg<sup>2+</sup>) declined 56.8% before and during the campaign. This suggests that the suspension of construction operations  
714 and increased frequency of rinsing and cleaning of paved roads significantly reduced dust emissions.

715       **(4) Regional linkage between surrounding areas played an important role.** PM<sub>2.5</sub> is a typical regional air  
716 pollutant, with obvious regional transport characteristics. In accordance with the requirements of the campaign  
717 scheme, eight cities around Jiaxing have actively implemented emissions reduction measures. During the campaign,  
718 PM<sub>2.5</sub> concentrations in eight surrounding cities and south-eastern Zhejiang also declined with obvious regional  
719 synergies.

720       It is worth noting that the implementation of control measures has also had a negative impact on the economy  
721 and the society in the short term while improving the air quality. For example, production restriction or suspension  
722 on a large number industrial enterprises were taken at great economic costs, and motor vehicle restriction had a  
723 large impact on the society.

724       **(5) Suggestions on emission reduction plans:** Local emission reductions shall be supplemented by regional  
725 linkage. Assessment results show that local emission reductions play a key role in ensuring air quality. Therefore,  
726 it is recommended that a synergistic emission reduction plan between adjacent areas with local pollution emission  
727 reductions as the core part should be established and strengthened, and emission reduction plans for different types  
728 of pollution through a stronger regional linkage should be reserved. Strengthen the pollution reduction in the upper  
729 reaches along the transport channel. It is especially crucial to enhance pollution emission reductions in the upper  
730 reaches of the channel since long-distance transport of plumes is a problem. This is especially true for key industrial  
731 sources and elevated sources. Considering that polluted air mass transport is more frequent in winter, it is necessary  
732 to develop emission reduction plans for different plume transport channels, combined with forecasting and warning  
733 mechanisms which could be initiated on time.

#### 734 **Author contribution**

735 L. Li designed this study and wrote the paper. H. L. Wang co-designed the study and provided valuable advice on  
736 the data analysis. C. Huang developed the regional emissions inventory. S. H. Zhu performed observational data  
737 analysis and J. Y. An carried out the CMAQ and CAMx modelling work. R. S. Yan performed the WRF modelling.  
738 M. Zhou and L. P. Qiao helped observation and data quality control. X. D. Tian and L. J. Shen carried out the  
739 measurements and provided the observed data. L. Huang and Y. J. Wang helped to revise the paper. Jeremy C. Aise  
740

741 and Joshua S Fu helped revise and polish the manuscript and gave advices on paper writing.

742 **Competing interests**

743 The authors declare that they have no conflict of interest.

744 **Acknowledgements.**

745 This study was financially supported by the “Chinese National Key Technology R&D Program” via grant No.  
746 2014BAC22B03 and the National Natural Science Foundation of China (NO. 41875161). We also thank the Joint  
747 pollution control office over the Yangtze River Delta region for co-ordinating the data share.

748 **References**

- 749 Appel, K.W., Bhave, P.V., Gilliland, A.B., Sarwar, G., Roselle, S.J.: Evaluation of the community multiscale air quality (CMAQ)  
750 model version 4.5: sensitivities impacting model performance; part II particulate matter. *Atmos. Environ.* 42, 6057-6066, 2008.
- 751 Borge, R., Lumbreiras, J., Vardoulakis, S., et al.: Analysis of long-range transport influences on urban PM10 using two-stage  
752 atmospheric trajectory clusters. *Atmos. Environ.*, 41, 4434-4405, 2007.
- 753 Burr, M. J., and Zhang, Y.: Source apportionment of fine particulate matter over the Eastern U.S. Part I: source sensitivity simulations  
754 using CMAQ with the Brute Force method, *Atmos. Pollut. Res.*, 2, 300-317, 2011.
- 755 Chen, P. L., Wang, T. J., Lu, X. B., et al.: Source apportionment of size-fractionated particles during the 2013 Asian Youth Games and  
756 the 2014 Youth Olympic Games in Nanjing, China, *Sci. Total Environ.*, 579,860-870, 2017.
- 757 Chen, Q., Fu, T. M., Hu, J., Ying, Q., & Zhang, L.: Modelling secondary organic aerosols in China. *National Science Review*, 4(6),  
758 806-809, 2017.
- 759 Chang, J. S., Brost, R. A., Isaksen, I. S. A., Madronich, S., Middleton, P., Stockwell, W. R., and Walcek, C. J.: A 3-DIMENSIONAL  
760 EULERIAN ACID DEPOSITION MODEL - PHYSICAL CONCEPTS AND FORMULATION, *J. Geophys. Res.*, 92, 14681-14700,  
761 1987.
- 762 Cheng, Y., Zheng, G., Wei, C., Mu, Q., Zheng, B., Wang, Z., Gao, M., Zhang, Q., He, K., Carmichael, G., Pöschl, U., and Su, H.:  
763 Reactive nitrogen chemistry in aerosol water as a source of sulfate during haze events in China, *Science Advances.*, 2, 1601530-  
764 1601530, doi:10.1126/sciadv.1601530, 2016.
- 765 Chou, M. D., and Suarez, M. J.: A solar radiation parameterization (CLIR-AD-SW) for atmospheric studies, 1999.
- 766 CAI-Asia.: “Blue Skies at Shanghai EXPO 2010 and Beyond: Analysis of Air Quality Management in Cities with Past and Planned  
767 Mega-Events: A Survey Report.” Pasig City, Philippines, 2010.
- 768 CAI-Asia.: “Nanjing YOG 2014 Home” Pasig City, Philippines, 2014.
- 769 Ek, M. B.: Implementation of Noah land surface model advances in the National Centers for Environmental Prediction operational  
770 mesoscale Eta model, *J. Geophys. Res.*, 108(D22), 2003.
- 771 Foley, K.M., Roselle, S.J., Appel, K.W., Bhave, P.V., Pleim, J.E., Otte, T.L., Mathur, R., Sarwar, G., Young, J.O., Gilliam, R.C., Nolte,

772 C.G., Kelly, J.T., Gilliland, A.B., Bash, J.O.: Incremental testing of the community multiscale air quality (CMAQ) modeling system  
773 version, 4.7. *Geosci. Model Dev.* 3, 205-226, 2010.

774 Fu, X., Cheng, Z., Wang, S., Hua, Y., Xing, J., and Hao, J.: Local and Regional Contributions to Fine Particle Pollution in Winter of  
775 the Yangtze River Delta, China, *Aerosol Air. Qual. Res.*, 16, 1067-1080, 2016.

776 Guenther, A. B., Jiang, X., Heald, C. L., Sakulyanontvittaya, T., Duhl, T., Emmons, L. K., and Wang, X.: The Model of Emissions of  
777 Gases and Aerosols from Nature version 2.1 (MEGAN2.1): an extended and updated framework for modeling biogenic emissions,  
778 *Geosci. Model Dev.*, 5, 1471-1492, 2012.

779 Grell, G. A., and Dévényi, D.: A generalized approach to parameterizing convection combining ensemble and data assimilation  
780 techniques, *Geophys. Res. Lett.*, 29(14), 587-590, 2002.

781 Han, X. K., Guo, Q. J., Liu, C. Q., et al.: Effect of the pollution control measures on PM<sub>2.5</sub> during the 2015 China Victory Day Parade:  
782 Implication from water-soluble ions and sulfur isotope, *Environ. Pollut.*, 218, 230-241, 2016.

783 Hu, J., Wang, P., Ying, Q., Zhang, H., Chen, J., Ge, X., et al.: Modeling biogenic and anthropogenic secondary organic aerosol in  
784 China. *Atmospheric Chemistry and Physics*, 17(1), 77-92, 2017.

785 Hu, J. L., Wang, Y. G., Ying, Q., et al.: Spatial and temporal variability of PM<sub>2.5</sub> and PM<sub>10</sub> over the North China Plain and the Yangtze  
786 River Delta, China, *Atmos. Environ.*, 95, 598-609, 2014.

787 Hu, J. L., Wu, Li., Zheng, B., et al.: Source contributions and regional transport of primary particulate matter in China, *Environ. Pollut.*,  
788 207, 31-42, 2015.

789 Hsu, Y. K., Holsen, T. M., and Hopke, P. K.: Comparison of hybrid receptor models to locate PCB sources in Chicago, *Atmos. Environ.*,  
790 37, 545-562, 2003.

791 Hong, S. Y.: A new vertical diffusion package with an explicit treatment of entrainment processes, *Mon. Weather Rev.*, 134, 2318,  
792 2006.

793 Huang, C., Chen, C. H., Li, L., Cheng, Z., Wang, H. L., Huang, H. Y., Streets, D. G., Wang, Y. J., Zhang, G. F., and Chen, Y. R.:  
794 Emission inventory of anthropogenic air pollutants and VOC species in the Yangtze River Delta region, China, *Atmos. Chem. Phys.*,  
795 11, 4105-4120, 2011.

796 Huang, Y. M., Liu, Y., Zhang, L. Y., et al.: Characteristics of Carbonaceous Aerosol in PM<sub>2.5</sub> at Wanzhou in the Southwest of China,  
797 *Atmosphere*, 9, 37, 2018.

798 Jiang, C., Wang, H., Zhao, T., et al.: Modeling study of PM<sub>2.5</sub> pollutant transport across cities in China's Jing-Jin-Ji region during a  
799 severe haze episode in December 2013, *Atmos. Chem. Phys.*, 15, 5803-5814, 2015.

800 Kang, H. Q., Zhu, B., Su, J. F., et al.: Analysis of a long-lasting haze episode in Nanjing, China, *Atmos. Res.*, 120-121, 78-87, 2013.

801 Kasibhatla, P., Chameides, W.L., Jonn, J.S.: A three dimensional global model investigation of seasonal variations in the atmospheric  
802 burden of anthropogenic sulphate aerosols. *J. Geophys. Res.* 102, 3737-3759, 1997.

803 Kelly, F. J., and Zhu, T.: Transport solutions for cleaner air, *Science*, 352, 934–936, 2016.

804 Li, J. L., ZHANG, M. G., GAO, Y., and CHEN, L.: Model analysis of secondary organic aerosol over China with a regional air quality  
805 modeling system (RAMS-CMAQ). *Atmospheric and Oceanic Science Letters*, 9(6), 443-450, 2016.

806 Li, L., An, J. Y., Zhou, M., Yan, R. S., Huang, C., Lu, Q., and Chen, C. H.: Source apportionment of fine particles and its chemical  
807 components over the Yangtze River Delta, China during a heavy haze pollution episode, *Atmos. Environ.*, 123, 415-429, 2015.

808 Li, R. P., Mao, H. J., Wu, L., et al.: The evaluation of emission control to PM concentration during Beijing APEC in 2014, *Atmos.*  
809 *Pollut. Res.*, 7 (2), 363-369, 2016.

810 Liu, H., Wang, X. M., Zhang, J. P., et al.: Emission controls and changes in air quality in Guangzhou during the Asian Games, *Atmos.*  
811 *Environ.*, 76, 81-93, 2013.

812 Lv, B. L., Liu, Y., Yu, P., et al.: Characterizations of PM<sub>2.5</sub> Pollution Pathways and Sources Analysis in Four Large Cities in China,  
813 *Aerosol Air Qual. Res.*, 15, 1836–1843, 2015.

814 Li, L., Chen, C. H., Fu, J. S., Huang, C., Streets, D. G., Huang, H. Y., and Fu, J. M.: Air quality and emissions in the Yangtze River  
815 Delta, China, *Atmos. Chem. Phys.*, 11(4), 1621-1639, 2011.

816 Liu, Y., Li, L., An, J. Y., Zhang, W., Yan, R. S., L. H., and M. W.: Emissions, chemical composition, and spatial and temporal allocation  
817 of the BVOCs in the Yangtze River Delta Region in 2014, *Environ. Sci.*, 39(2), 2018.

818 Li, M., Zhang, Q., Kurokawa, J.-i., Woo, J.-H., He, K., Lu, Z., and Zheng, B.: MIX: a mosaic Asian anthropogenic emission inventory  
819 under the international collaboration framework of the MICS-Asia and HTAP, *Atmos. Chem. Phys.*, 17(2), 935-963, 2017.

820 Lin, Y. L.: Bulk parameterization of the snow field in a cloud model, *J. Appl. Meteorol.*, 22(6), 1065-1092, 1983.

821 Li, L., Chen, C. H., Fu, J. S., Huang, C., Streets, D. G., Huang, H. Y., Zhang, G. F., Wang, Y. J., Jang, C. J., Wang, H. L., Chen, Y. R.,  
822 and Fu, J. M.: Air quality and emissions in the Yangtze River Delta, China, *Atmos. Chem. Phys.*, 11, 1621-1639, 2011.

823 Li, L., An, J. Y., Zhou, M., Yan, R. S., Huang, C., Lu, Q., Lin, L., Wang, Y. J., Tao, S. K., Qiao, L. P., Zhu, S. H., and Chen, C. H.:  
824 Source apportionment of fine particles and its chemical components over the Yangtze River Delta, China during a heavy haze  
825 pollution episode, *Atmos. Environ.*, 123, 415-429, 2015.

826 Li, M., Zhang, Q., Kurokawa, J.-i., Woo, J.-H., He, K., Lu, Z., Ohara, T., Song, Y., Streets, D. G., Carmichael, G. R., Cheng, Y., Hong,  
827 C., Huo, H., Jiang, X., Kang, S., Liu, F., Su, H., and Zheng, B.: MIX: a mosaic Asian anthropogenic emission inventory under the  
828 international collaboration framework of the MICS-Asia and HTAP, China, *Atmos. Chem. Phys.*, 17, 935-963, 2017.

829 Li, X., Zhang, Q., Zhang, Y., Zheng, B., Wang, K., Chen, Y., Wallington, T. J., Han, W., Shen, W., Zhang, X., and He, K.: Source  
830 contributions of urban PM 2.5 in the Beijing–Tianjin–Hebei region: Changes between 2006 and 2013 and relative impacts of  
831 emissions and meteorology, *Atmos. Environ.*, 123, 229-239, 2015.

832 Lin, Y. L.: Bulk parameterization of the snow field in a cloud model, *J. Appl. Meteorol.*, 22, 1065-1092, 1983.

833 Liu, Y., Li, L., An, J. Y., Zhang, W., Yan, R. S., L. H., Huang, C., Wang, H. L., Q. W., and M. W.: Emissions, chemical composition,

834 and spatial and temporal allocation of the BVOCs in the Yangtze River Delta Region in 2014, *Environ. Sci.*, 39, 608-617, 2018.

835 Liang, P. F., Zhu, T., Fang, Y. H., Li, Y. R., Han, Y. Q., Wu, Y. S., Hu, M., and Wang, J. X.: The role of meteorological conditions  
836 and pollution control strategies in reducing air pollution in Beijing during APEC 2014 and Victory Parade 2015, *Atmos. Chem.*  
837 *Phys.*, 17, 13921–13940, 2017.

838 Liu, J., and Zhu, T.: NO<sub>x</sub> in Chinese Megacities, *Nato. Sci. Peace. Secur.*, 120, 249–263, 2013.

839 [Lu, Q. L., Zhang, Y. F., Ma, Y. H., et al.: Source identification of trace elements in the atmosphere during the second Asian Youth  
840 Games in Nanjing, China: Influence of control measures on air quality, \*Atmos. Pollut. Res.\*, 7 \(3\), 547-556, 2016.](#)

841 Markovic, M. Z., VandenBoer, T.C., and Murphy, J. G.: Characterization and Optimization of an Online System for the Simultaneous  
842 Measurement of Atmospheric Water-soluble Constituents in the Gas and Particle Phases, *J. Environ. Monit.*, 14, 1872–1874, 2012.

843 Mlawer, E. J., Taubman, S. J., Brown, P. D., Iacono, M. J., and Clough, S. A.: Radiative transfer for inhomogeneous atmospheres:  
844 RRTM, a validated correlated-k model for the longwave, *J. Geophys. Res.*, 102(D14), 16663-16682, 1997.

845 Nolte, C. G., Appel, K. W., Kelly, J. T., Bhawe, P. V., Fahey, K. M., Collet Jr., J. L., Zhang, L., and Young, J. O.: Evaluation of the  
846 Community Multiscale Air Quality (CMAQ) model v5.0 against size-resolved measurements of inorganic particle composition  
847 across sites in North America, *Geosci. Model Dev.*, 8, 2877-2892, 2015.

848 Nenes, A., Pilinis, C., and Pandis, S. N.: ISORROPIA: A New Thermodynamic Model for Multiphase Multicomponent Inorganic  
849 Aerosols, *Aquat. Geochem.*, 4, 123-152, 1998.

850 Pui, D. Y. H., Chen, S. C., and Zuo, Z. L.: PM<sub>2.5</sub> in China: Measurements, sources, visibility and health effects, and mitigation,  
851 *Particuology*, 13, 1-26, 2014.

852 Polissar, A. V., Hopke, P. K., Kaufmann, P. P., Kaufmann, Y., Hall, D., Bodhaine, B., Dutton, E., and Harris J.: The aerosol at Barrow,  
853 Alaska: long-term trends and source location, *Atmos. Environ.*, 33(16), 2441-2458, 1999.

854 [Qi, L., Zhang, Y. F., Ma, Y. H., et al.: Source identification of trace elements in the atmosphere during the second Asian Youth Games  
855 in Nanjing, China: Influence of control measures on air quality, \*Atmos. Pollut. Res.\*, 7 \(3\), 547-556, 2016.](#)

856 Swagata, P., Pramod, K., Sunita, V., et al.: Potential source identification for aerosol concentrations over a site in Northwestern India,  
857 *Atmos. Res.*, 169, 65-72, 2016.

858 Sun, Y. L., Wang, Z. F., Wild, O., et al.: “APEC Blue”: Secondary Aerosol Reductions from Emission Controls in Beijing, *Sci. Rep-  
859 UK.*, 6, 20668, 2016.

860 Tang, L., Haeger-Eugensson, M., Sjoberg, K., et al.: Estimation of the long-range transport contribution from secondary inorganic  
861 components to urban background PM<sub>10</sub> concentrations in south-western Sweden during 1986-2010, *Atmos. Environ.*, 89, 93-101,  
862 2014.

863 Tang, G., Zhu, X., Hu, B. et al.: Impact of emission controls on air quality in Beijing during APEC 2014: lidar ceilometer observations,  
864 *Atmos. Chem. Phys.*, 15, 12667–12680, 2015.



865 Tian, Mi., Wang, H. B., Chen, Y., et al.: Characteristics of aerosol pollution during heavy haze events in Suzhou, China, *Atmos. Chem.*  
866 *Phys.*, 16, 7357–7371, 2016.

867 US EPA.: Draft Modeling Guidance for Demonstrating Attainment of Air Quality Goals for Ozone, PM<sub>2.5</sub>, and Regional Haze, 2014.

868 Wang, L. T., Wei, Z., Yang, J., Zhang, Y., Zhang, F. F., Su, J., Meng, C. C., and Zhang, Q.: The 2013 severe haze over southern Hebei,  
869 China: model evaluation, source apportionment, and policy implications, *Atmos. Chem. Phys.*, 14, 3151-3173, 2014.

870 Wang, Y. Q., Zhang, X. Y., and Draxler, R. R.: TrajStat: GIS-based software that uses various trajectory statistical analysis methods  
871 to identify potential sources from long-term air pollution measurement data, *Environ. Modell. Softw.*, 24(8), 938-939, 2009.

872 West, J. J., Cohen, A., Dentener, F., Brunekreef, B., Zhu, T., Armstrong, B., Bell, M. L., Brauer, M., Carmichael, G., Costa, D. L.,  
873 Dockery, D. W., Kleeman, M., Krzyzanowski, M., Künzli, N., Liousse, C., Lung, S. C., Martin, R. V., Pöschl, U., Pope, C. A.,  
874 Roberts, J. M., Russell, A. G., and Wiedinmyer, C.: “What We Breathe Impacts Our Health: Improving Understanding of the Link  
875 between Air Pollution and Health”, *Environ. Sci. Technol.*, 50 (10), 4895–4904, 2016.

876 Wang, T., Nie, W., Gao, J., et al.: Air quality during the 2008 Beijing Olympics: secondary pollutants and regional impact, *Atmos.*  
877 *Chem. Phys.*, 10, 7603–7615, 2010.

878 Wang, Y., Hao, J., McElroy, M. B., et al.: Ozone air quality during the 2008 Beijing Olympics: effectiveness of emission restrictions,  
879 *Atmos. Chem. Phys.*, 9, 5237–5251, 2009.

880 Wang Y Q, Zhang X Y, Draxler R R. TrajStat: GIS-based software that uses various trajectory statistical analysis methods to identify  
881 potential sources from long-term air pollution measurement data. *Environmental Modelling and Software*, 24(8): 938-939, 2009.

882 Wang, Y. Q., Zhang, Y., Schauer, J. J., et al.: Relative impact of emissions controls and meteorology on air pollution mitigation  
883 associated with the Asia-Pacific Economic Cooperation (APEC) conference in Beijing, China, *Sci. Total Environ.*, 571, 1467-1476,  
884 2016.

885 Wang, Z. S., Li, Y. T., Chen, T., et al.: Changes in atmospheric composition during the 2014 APEC conference in Beijing, *J. Geophys.*  
886 *Res.*, 120 (24), 2015.

887 Wang, Q. Z., Zhuang, G. S., Huang, Kan., et al.: Probing the severe haze pollution in three typical regions of China: Characteristics,  
888 sources and regional impacts, *Atmos. Environ.*, 120, 76-88, 2015.

889 Xu, W., Song, Wei., Zhang, Y. Y., et al.: Air quality improvement in a megacity: implications from 2015 Beijing Parade Blue pollution  
890 control actions, *Atmos. Chem. Phys.*, 17, 31–46, 2017.

891 Xiao, Z. M., Zhang, Y. F., Hong, S. M., et al.: Estimation of the Main Factors Influencing Haze, Based on a Long-term Monitoring  
892 Campaign in Hangzhou, China, *Aerosol Air Qual. Res.*, 11, 873–882, 2011.

893 Yang, H. N., Chen, J., Wen, J. J., et al.: Composition and sources of PM<sub>2.5</sub> around the heating periods of 2013 and 2014 in Beijing:  
894 Implications for efficient mitigation measures, *Atmos. Environ.*, 124, 378-386, 2016.

895 Yu, S. C., Saxena, V. K., Zhao, Z.: A comparison of signals of regional aerosol-induced forcing in eastern China and the southeastern

896 United States, *Geophys. Res. Lett.*, 28, 713-716, 2001.

897 Yu, S. C., Zhang, Q. Y., Yan, R. C., et al.: Origin of air pollution during a weekly heavy haze episode in Hangzhou, China, *Environ.*  
898 *Chem. Lett.*, 12, 543-550, 2014.

899 Yarwood, G., Rao, S., Yocke, M., et al.: Updates to the Carbon Bond chemical mechanism: CB05, Final Report prepared for US EPA,  
900 2005.

901 Zhang, Y., Cheng, S. H., Chen, Y. S., and Wang, W. X.: Application of MM5 in China: Model evaluation, seasonal variations, and  
902 sensitivity to horizontal grid resolutions, *Atmos. Environ.*, 45, 3454-3465, 2011.

903 Zheng, B., Zhang, Q., Zhang, Y., He, K. B., Wang, K., Zheng, G. J., Duan, F. K., Ma, Y. L., and Kimoto, T.: Heterogeneous chemistry:  
904 a mechanism missing in current models to explain secondary inorganic aerosol formation during the January 2013 haze episode in  
905 North China, *Atmos. Chem. Phys.*, 15, 2031-2049, 2015.

906 Zeng, Y., and Hopke, P. K.: A study of the sources of acid precipitation in Ontario, Canada, *Atmos. Environ.*, 23(7), 1499-1509, 1989.

907 Zhang, X. Y., Wang, Y. Q., Niu, T., et al.: Atmospheric aerosol compositions in China: spatial/temporal variability, chemical signature,  
908 regional haze distribution and comparisons with global aerosols, *Atmos. Chem. Phys.*, 12, 779-799, 2012.

909 Zhang, Y. J., Tang, L. L., Wang, Z., et al.: Insights into characteristics, sources, and evolution of submicron aerosols during harvest  
910 seasons in the Yangtze River delta region, China, *Atmos. Chem. Phys.*, 15, 1331-1349, 2015.